High order linearly implicit methods
for semilinear evolution PDEs

Guillaume Dujardin & Ingrid Lacroix-Violet

High order linearly implicit methods for semilinear evolution PDEs

Guillaume Dujardin [1]
Ingrid Lacroix-Violet [2]

[1] Univ. Lille, Inria, CNRS, UMR 8524 - Laboratoire Paul Painlevé F-59000 Lille, France
E-mail address: guillaume.dujardin@inria.fr
[2] Université de Lorraine, CNRS, IECL, F-54000 Nancy, France
E-mail address: ingrid.lacroix@univ-lorraine.fr.

Abstract. This paper considers the numerical integration of semilinear evolution PDEs using the high order linearly implicit methods developed in [21] in the ODE setting. These methods use a collocation Runge–Kutta method as a basis, and additional variables that are updated explicitly and make the implicit part of the collocation Runge–Kutta method only linearly implicit. In this paper, we introduce several notions of stability for the underlying Runge–Kutta methods as well as for the explicit step on the additional variables necessary to fit the context of evolution PDE. We prove a main theorem about the high order of convergence of these linearly implicit methods in this PDE setting, using the stability hypotheses introduced before. We use nonlinear Schrödinger equations and heat equations as main examples but our results extend beyond these two classes of evolution PDEs. We illustrate our main result numerically in dimensions 1 and 2, and we compare the efficiency of the linearly implicit methods with other methods from the literature. We also illustrate numerically the necessity of the stability conditions of our main result.

2020 Mathematics Subject Classification. 65M12, 65M22, 65M70, 35K05, 35K58, 35Q55.

Keywords. numerical analysis; high order methods; linearly implicit methods; collocation methods; Runge–Kutta methods; NLS equation; heat equation.

1. Introduction

High order linearly implicit methods for the time integration of evolution problems have been derived, analysed and implemented recently in [21]. In the context of evolution ODEs, [21] provides sufficient and constructive conditions to achieve any arbitrarily high order with such methods. The goal of this paper is to extend the design and analysis of such methods to the case of semilinear evolution PDEs, that we semi-discretize in time. We mostly focus on nonlinear Schrödinger equations (NLS) and nonlinear heat equations (NLH), even if the analysis can also be extended to other semilinear equations of the form

$$\partial_t u(t, \mathbf{x}) = Lu(t, \mathbf{x}) + N(u(t, \mathbf{x}))u(t, \mathbf{x}), \qquad t \geq 0, \mathbf{x} \in \Omega, \tag{1.1}$$

where L is an unbounded linear operator on some Banach space X of functions on some Ω with appropriate boundary conditions. The function N is a nonlinear function of the unknown u from X to itself. The unknown u is a real or complex-valued function of time $t \geq 0$ and space $\mathbf{x} \in \Omega$. The autonomous evolution equation (1.1) is supplemented with an initial condition at $t = 0$. More precise hypotheses and their corresponding functional framework are introduced below. For example, denoting by Δ the usual Laplace operator, the cubic NLS may correspond to $N(u) = iq|u|^2$ (for some $q \in \mathbb{R}$) and $L = i\Delta$, and the cubic NLH may correspond to $L = \Delta$ and $N(u) = \pm|u|^2$. In classical cases depending on the geometry of Ω and the choice of boundary conditions (e.g. $\Omega = \mathbb{R}^d$ or $\Omega = (\mathbb{R}/\mathbb{Z})^d = \mathbb{T}^d$), and the choice of X, the localization of the spectrum of L is known. Indeed, the spectrum of L lies on the

purely imaginary axis for NLS, and in the left hand side of the complex plane for NLH. In particular, we provide in this paper sufficient conditions to achieve any arbitrarily high order with linearly implicit methods for the NLS and NLH equations. Our results of course extend to other semilinear evolution PDEs.

The numerical integration of such problems has a long history, and numerical schemes have been derived and analysed in several contexts. For the NLS equation, let us mention for example [17] and [23] where the Crank–Nicolson scheme is studied, [35] where the Lie–Trotter split step method is introduced, [2] where some Runge–Kutta methods are used with Galerkin space discretization, [6] where a relaxation method is introduced, which is proved to be of order 2 in [9]. Methods with higher order in time, for example exponential methods [10, 20] or splitting methods (see [7, 31] for error estimates), have also been designed and studied. The numerical behaviour in the semiclassical limit has also been studied [8, 29]. For the NLH equation, one may mention Crank–Nicolson [3] as well as splitting methods [13, 18, 19], exponential methods [27] [28], including Lawson and exponential Runge–Kutta methods.

Some of these methods are fully implicit (e.g. Crank–Nicolson), some are fully explicit (e.g. a Lawson method based on an explicit Runge–Kutta method), and some are linearly implicit (e.g. for the NLS equation, the relaxation scheme of [6]; for nonlinear parabolic equations, the linearly implicit Rosenbrock methods and W-methods analysed in [32], the linearly implicit multistep methods analysed in [1], the IMEX schemes analysed in [12]). In some sense, the methods proposed and analysed in this paper appear as generalizations of the relaxation method of [6], and form a new class (introduced in [21]) of linearly implicit methods, different from the ones listed above. Indeed, they are linearly implicit : at the cost of introducing extra variables, they require only the solution of one linear system per time step so that they do not require CFL conditions to ensure stability that usually appear in explicit methods. Of course, the solution of one high dimensional linear system per time step has a computational cost, when compared to other high order methods. For the solution of such a system, one may rely on very efficient techniques, either direct (LU factorization, Choleski factorization, etc.) or iterative (Jacobi method, Gauss–Seidel method, conjugate gradient, Krylov subspace method, etc. [33]), depending on the structure of the problem at hand. Depending on the problem, linearly implicit methods can outperform high order methods from the literature. In particular, the linearly implicit methods below can be competitive when the spectrum of the linear operator L is unknown (only the localization of the spectrum in the complex plane matters, in some sense), while exponential methods may be faster for problems where that spectrum is known. An example can be found in Section 3.2.2 of [21] for an NLS equation on a domain where the spectrum of the Laplace operator is not known and a linearly implicit method of order 2 belonging to the class studied below outperforms the Strang splitting method.

Other authors have considered adding extra variables for the time integration of evolution problems. For example, [14, 34] introduced scalar auxiliary variable methods (SAV) and multiple scalar auxiliary variable methods (MSAV). These methods were introduced to produce unconditionaly stable schemes for dissipative problems with gradient flow structure. The auxiliary variables in this context are used to ensure discrete energy decay. The order of the methods (1 or 2 in the references above) was not the main issue. In contrast, the linearly implicit methods analysed in this paper achieve arbitrarily high order in time.

The reader may refer to the Introduction section of [21] for the comparison of the linearly implicit methods introduced there and analysed here in a PDE context, and other classical time integration methods from the literature (one-step methods, including Runge–Kutta methods, linear multistep methods, composition methods, etc.).

The linearly implicit methods of [21], that we further analyse below for NLS and NLH equations, embed a classical collocation Runge–Kutta method with additional variables, in the spirit of the relaxation method introduced by Besse [6]. The analysis of the convergence of these linearly implicit

methods applied to semilinear problems like NLS and NLH relies on stability hypotheses of two different kinds : on the classical collocation Runge–Kutta method used on the one hand, and on the explicit update formula for the additional variables. For the stability of the Runge–Kutta method itself, we refer to the work of Crouzeix and Raviart [15, 16]. In this paper, we generalize some stability notions defined in these works (see Definition 3.4 below and also [22]), that allow to ensure global stability of our linearly implicit methods. For the stability of the explicit update of the additional variables, we extend results of [21] in the ODE case to the PDE (1.1).

This paper is organized as follows. Section 2 describes the extension of the linearly implicit methods of [21] to the PDE setting. First, we adapt in Section 2.1.1 the classical Runge–Kutta framework for ODEs to the PDE context. This allows for a description of the linearly implicit methods in the PDE setting in Section 2.1.2. In Section 2.2, we introduce the functional framework that allows to ensure the stability of the explicit update of the additional variables (Lemma 2.4). In Section 3, we analyse the consistency and convergence errors of the linearly implicit methods in Section 3.1, and the stability of the linear Runge–Kutta step in Section 3.2. This allows for exposing our hypotheses on the exact solution of (1.1) as well as on the numerical parameters in Section 3.3 to ensure in our main result (Theorem 3.12) that linearly implicit methods actually converge with high order. The proof of the theorem is provided in Section 3.4. Section 4 is devoted to proving that for the NLS equation, the Cooper condition on the coefficients of the underlying collocation Runge–Kutta method ensures that the mass is preserved by the linearly implicit numerical method. We provide numerical experiments in Section 5. We consider NLS equations in 1D (methods of order 2 in Section 5.2.1, methods of order 4 in Section 5.2.2 and a method of order 5 in Section 5.2.3) and in 2D on a star-shaped domain (see Section 5.3). We consider NLH equations in 1D (methods of order 2 in Section 5.4). In all these cases, we illustrate numerically the main result of the paper (Theorem 3.12) and we compare the precision and efficiency of the high order linearly implicit methods with that of other methods from the literature. We also demonstrate numerically in Section 5 the necessity of our stability hypotheses in the PDE setting. Section 6 conludes this paper and introduces future works. An appendix is proposed in Section 7, which includes proofs of several technical results (Sections 7.1 and 7.2) as well as Butcher's tableaux of the underlying Runge–Kutta methods used in this paper for the numerical experiments of Section 5 to allow for reproducibility of the numerical results.

2. **Linearly implicit methods for semilinear evolution PDEs**

In this section, we introduce the linearly implicit methods from [21] adapted to the PDE setting of the equation (1.1) as well as the associated functional framework.

2.1. **Description of the linearly implicit methods**

Linearly implicit method from [21] applied to a semilinear PDE of the form (1.1) rely on a classical Runge–Kutta method, referred to as the "underlying Runger–Kutta method" in the following, as well as on additional variables that are explicitly updated at every time step. Before adapting the definition of the linearly implicit methods from [21] to the PDE context at hand in 2.1.2, we recall some basic notations for classical Runge–Kutta methods applied to PDE problems and introduce their (linear) stability function in Section 2.1.1.

2.1.1. *The underlying Runge–Kutta method*

We consider throughout this paper a Runge–Kutta method with a fixed number $s \in \mathbb{N}^\star$ of stages, and real coefficients $(a_{ij})_{1 \leq i,j \leq s}$, $(b_i)_{1 \leq i \leq s}$, $(c_i)_{1 \leq i \leq s}$. We group these coefficients in a square matrix A of size s with coefficients $(a_{i,j})_{1 \leq i,j \leq s}$, a column vector b of size s with coefficients $(b_i)_{1 \leq i \leq s}$, and a

column vector c of size s with coefficients $(c_i)_{1 \leq i \leq s}$. We moreover denote by $\mathbb{1}$ the column vector of size s with all components equal to 1. We recall that the (linear) stability function of the method is defined for $\lambda \in \mathbb{C}$ by

$$R(\lambda) = 1 + \lambda b^t (I - \lambda A)^{-1} \mathbb{1}, \tag{2.1}$$

where I is the identity matrix of size s. Note that the function R is a rational function of λ. We denote by $A \otimes L$ the operator-valued matrix

$$A \otimes L = \begin{pmatrix} a_{11}L & \dots & a_{1s}L \\ \vdots & & \vdots \\ a_{s1}L & \dots & a_{ss}L \end{pmatrix}.$$

Similarly, we set

$$b^t \otimes L = (b_1 L, \dots, b_s L).$$

The notation I will be used for the identity operator in general.

2.1.2. *Linearly implicit methods*

We follow the methods introduced in an ODE context in [21] and we consider some $h > 0$ as a time step. Since the problem (1.1) is autonomous, we always consider $t = 0$ as the starting time without loss of generality. We take $u^0 \in H^\sigma$ (classical Sobolev space of order σ, to be defined in the next section), and we denote by $t \mapsto u(t)$ the exact solution of (1.1) with initial datum $u(0) = u^0$. Of course, for fixed $t \geq 0$, the function $u(t)$ is itself a function of $\mathbf{x} \in \Omega$. We will often omit this dependency in the notations. We initialize the linearly implicit method with $u_0 \in H^\sigma$, close to u^0. We initialize the additional variables $(\gamma_{-1,i})_{1 \leq i \leq s}$ with approximations of $(N(u((c_i-1)h)))_{1 \leq i \leq s}$ and we set $\Gamma_{-1} = (\gamma_{-1,i})_{1 \leq i \leq s}^t \in (H^\sigma)^s$. The question of the precomputation of these initial values of the additional variables is addressed in Remark 2.11 in [21]. Assuming one knows an approximation u_n of the exact solution u at time $t_n = nh$ and approximations $\Gamma_{n-1} = (\gamma_{n-1,i})_{1 \leq i \leq s}$ of $(N(u(t_{n-1} + c_i h)))_{1 \leq i \leq s}$ for some integer $n \geq 0$, the first step of a linearly implicit method as introduced in [21] consists in computing pointwise in $\mathbf{x}$

$$\Gamma_n = D\Gamma_{n-1} + \Theta N(u_n), \tag{2.2}$$

where D is a given $s \times s$ real or complex matrix and $\Theta = (\theta_1, \dots, \theta_s)^t$ is a given real or complex column vector, that are part of the method and do not depend on n. Let us recall a definition from [21].

Definition 2.1. The step (2.2) is said to be strongly stable when the spectral radius $\rho(D)$ of the matrix D is stricly smaller than 1. It is said to be consistent of order s when it satisfies

$$V_c = DV_{c-\mathbb{1}} + \vartheta, \tag{2.3}$$

where V_c is the Vandermonde matrix at points $(c_1, \dots, c_s)$ (i.e. $(V_c)_{i,j} = c_i^{j-1}$ for all i, j), $V_{c-\mathbb{1}}$ is the Vandermonde matrix at points $(c_1 - 1, \dots, c_s - 1)$ (i.e. $(V_{c-\mathbb{1}})_{i,j} = (c_i - 1)^{j-1}$ for all i, j), and ϑ is an $s \times s$ matrix with Θ as first column and zero everywhere else.

The fact that Equation (2.2) provides a good approximation of $N(u)$, provided that D and Θ satisfy (2.3), appears in the proof of Proposition 3.2 in the PDE context just as it did in the ODE context of [21]. Existence of matrices D and vectors Θ, such that the step (2.2) is strongly stable and consistent of order s is discussed in [21], and formulas are provided as well. In this paper, we will always assume that the step (2.2) is strongly stable and is consistent of order s. The second step of the linearly implicit method uses the Runge–Kutta method introduced in 2.1.1 in the following way. One first solves for $(u_{n,i})_{1 \leq i \leq s}$ the following $s \times s$ linear system

$$u_{n,i} = u_n + h \sum_{j=1}^{s} a_{ij}(L + \gamma_{n,j})u_{n,j} \qquad 1 \leq i \leq s. \tag{2.4}$$

Setting $U_n \in (H^\sigma)^s$ as the unknown vector with components $(u_{n,i})_{1 \le i \le s}$, the system (2.4) reads

$$(I - hA \otimes L)U_n = u_n \mathbb{1} + hA(\Gamma_n \bullet U_n), \tag{2.5}$$

where $\Gamma_n \bullet U_n$ denotes the column vector with components $(\gamma_{n,i} u_{n,i})_{1 \le i \le s}$, which is the componentwise column vector product of Γ_n and U_n. Afterwards, the third and last step of the linearly implicit method consists in computing explicitly

$$u_{n+1} = u_n + h \sum_{i=1}^{s} b_i (L + \gamma_{n,i}) u_{n,i}. \tag{2.6}$$

This last step can be also written

$$u_{n+1} = u_n + h \left(b^t \otimes L \right) U_n + h b^t (\Gamma_n \bullet U_n). \tag{2.7}$$

Definition 2.2 (collocation methods). The Runge–Kutta method defined by A, b and c is said to be of collocation when $c_1, c_2, \ldots, c_s$ are distinct real numbers and A and b satisfy for all $(i, j) \in \{1, \ldots, s\}^2$,

$$a_{ij} = \int_0^{c_i} \ell_j(\tau) \mathrm{d}\tau \qquad \text{and} \qquad b_i = \int_0^1 \ell_i(\tau) \mathrm{d}\tau, \tag{2.8}$$

where $(\ell_i)_{1 \le i \le s}$ are the s Lagrange polynomials associated to $(c_1, \ldots, c_s)$ defined by

$$\forall i \in \{1, \ldots, s\}, \qquad \ell_i(\tau) = \prod_{\substack{j \ne i \\ j=1}}^{s} \frac{(\tau - c_j)}{(c_i - c_j)}. \tag{2.9}$$

Remark 2.3. In the examples of this paper, we shall order the coefficients $c_1, \ldots, c_s$ in such a way that $c_1 < \cdots < c_s$ and assume that they all lie in $[0, 1]$.

2.2. Functional framework

In this paper, for expository purposes, we consider the case $\Omega = \mathbb{R}^d$ in particular in the proofs of our results. In this case, we denote by H^σ the space of functions f from $\mathbb{R}^d$ to $\mathbb{C}$ such that

$$\int_{\mathbb{R}^d} |\hat{f}(\xi)|^2 (1 + |\xi|^2)^\sigma \mathrm{d}\xi < +\infty,$$

equipped with the norm $\|f\|_{H^\sigma} = \left(\int_{\mathbb{R}^d} |\hat{f}(\xi)|^2 (1 + |\xi|^2)^\sigma \mathrm{d}\xi \right)^{\frac{1}{2}}$, where $\hat{f}$ stands for the Fourier transform of the function f. The corresponding norm on $(H^\sigma)^s$ is defined for $F = (f_1, \ldots, f_s)^t$ in $(H^\sigma)^s$ by

$$\|F\|_{(H^\sigma)^s} = \left(\sum_{p=1}^{s} \int_{\mathbb{R}^d} |\hat{f}_p(\xi)|^2 (1 + |\xi|^2)^\sigma \mathrm{d}\xi \right)^{\frac{1}{2}}. \tag{2.10}$$

Of course, our results extend to several other cases. Let us mention two of them : the d-dimensional torus $\Omega = \mathbb{T}^d$ and the case of a bounded open set Ω with a Lipschitz boundary and homogeneous Dirichlet boundary conditions. First, in the case of the torus $\mathbb{T}^d$, we denote by H^σ the space of functions f from $\mathbb{T}^d$ to $\mathbb{C}$ such that

$$\sum_{k \in \mathbb{Z}^d} |\hat{f}(k)|^2 (1 + |k|^2)^\sigma < +\infty,$$

equipped with the norm $\|f\|_{H^\sigma} = \left(\sum_{k \in \mathbb{Z}^d} |\hat{f}(k)|^2 (1 + |k|^2)^\sigma \right)^{\frac{1}{2}}$, where $\hat{f}$ stands for the sequence of Fourier coefficients of f. The corresponding norm on $(H^\sigma)^s$ is defined for $F = (f_1, \ldots, f_s)^t \in (H^\sigma)^s$ by

$$\|F\|_{(H^\sigma)^s} = \left(\sum_{p=1}^{s} \sum_{k \in \mathbb{Z}^d} |\hat{f}_p(k)|^2 (1 + |k|^2)^\sigma \right)^{\frac{1}{2}}. \tag{2.11}$$

Second, in the case of a bounded open set Ω with a Lipschitz boundary, the Laplace operator with homogeneous Dirichlet boundary conditions has compact inverse. Hence its spectrum consists in a countable set of negative eigenvalues $(-\lambda_k^2)_{k\in\mathbb{N}}$ with $\lambda_k > 0$ and $\lambda_k \underset{k\to+\infty}{\longrightarrow} +\infty$, and there exists an orthogonal Hilbert basis $(e_k)_{k\in\mathbb{N}}$ of $L^2(\Omega)$ consisting in eigenvectors of this Laplace operator. Indeed, the integration by parts formula holds true in this case (see Theorem 2.4.1 in [30]) and this allows to perform the usual variational analysis (see Theorem 7.3.2 in [4]). We denote by H^σ the space of functions $f \in L^2(\Omega, \mathbb{C})$ such that

$$\sum_{k\in\mathbb{N}} |\alpha_k|^2 (1 + \lambda_k^2)^\sigma < +\infty,$$

where $f = \sum_{k=0}^{+\infty} \alpha_k e_k$. Of course, the associated norm on H^σ is defined by

$$\|f\|_{H^\sigma} = \left(\sum_{k\in\mathbb{N}} |\alpha_k|^2 (1 + \lambda_k^2)^\sigma \right)^{\frac{1}{2}},$$

and that on $(H^\sigma)^s$ is defined for $F = (f_1, \ldots, f_s)^t \in (H^\sigma)^s$ by

$$\|F\|_{(H^\sigma)^s} = \left(\sum_{p=1}^{s} \sum_{k\in\mathbb{N}} |\alpha_k^p|^2 (1 + \lambda_k^2)^\sigma \right)^{\frac{1}{2}}, \tag{2.12}$$

where for all $p \in \{1, \ldots, s\}$, $f_p = \sum_{k=0}^{+\infty} \alpha_k^p e_k$.

In all cases, we chose $\sigma > d/2$ so that H^σ is an algebra. This is well known for $\Omega = \mathbb{R}^d$ and $\Omega = \mathbb{T}^d$, and holds for Ω bounded open set of $\mathbb{R}^d$ with Lipschitz boundary (see for example after Theorem 1.4.4.2 in [24]). Of course, one can even think of more general settings allowing for the algebra property on H^σ (see for example [5] and references therein), but we will not do so in this paper.

The norm of linear continuous operators from H^σ to itself is denoted by $\|\cdot\|_{H^\sigma \to H^\sigma}$, and that of $(H^\sigma)^s$ to itself is denoted by $\|\cdot\|_{(H^\sigma)^s \to (H^\sigma)^s}$.

Lemma 2.4. *As above, assume D is a complex $s \times s$ matrix. The linear mapping $F \mapsto DF$ sends $(H^\sigma)^s$ to itself continuously. Moreover, if the step (2.2) is strongly stable (i.e. $\rho(D) < 1$), then for all $\delta \in (\rho(D), 1)$, there exists a norm $\|\cdot\|_{(H^\sigma)^s, D}$ on $(H^\sigma)^s$, equivalent to the usual norm defined above (in 2.10, 2.11 or 2.12), such that*

$$\forall F \in (H^\sigma)^s, \qquad \|DF\|_{(H^\sigma)^s, D} \leq \delta \|F\|_{(H^\sigma)^s, D}. \tag{2.13}$$

Proof. We prove the result in the case of the full space $\mathbb{R}^d$. The proof in the other cases follows the same lines. First, one can check that

$$\forall F \in (H^\sigma)^s, \quad \forall \xi \in \mathbb{R}^d, \qquad \widehat{DF}(\xi) = D\hat{F}(\xi). \tag{2.14}$$

Therefore,

$$\forall F \in (H^\sigma)^s, \qquad \|DF\|_{(H^\sigma)^s} \leq C \|F\|_{(H^\sigma)^s},$$

where C is any constant greater or equal to the norm of the matrix D as a continuous linear operator from the hermitian space $\mathbb{C}^s$ to itself. If we assume moreover that $\rho(D) < 1$ and $\delta \in (\rho(D), 1)$ is given, then one can chose $\varepsilon > 0$ sufficiently small to ensure that $\rho(D) + \varepsilon \leq \delta$. Denoting by $|\cdot|_D$ the norm on $\mathbb{C}^s$ provided by Lemma 7.2, we can define a norm on $(H^\sigma)^s$ by setting

$$\forall F \in (H^\sigma)^s, \qquad \|F\|_{(H^\sigma)^s, D} = \left(\int_{\mathbb{R}^d} |\hat{F}(\xi)|_D^2 (1 + |\xi|^2)^\sigma \mathrm{d}\xi \right)^{\frac{1}{2}}.$$

Since $|\cdot|_D$ is equivalent to the usual hermitian norm on $\mathbb{C}^s$, the norm $\|\cdot\|_{(H^\sigma)^s,D}$ is equivalent to the norm $\|\cdot\|_{(H^\sigma)^s}$. Moreover, thanks to (2.14) and Lemma 7.2, one has

$$\forall F \in (H^\sigma)^s, \qquad \|DF\|^2_{(H^\sigma)^s,D} = \int_{\mathbb{R}^d} |D\hat{F}(\xi)|^2_D (1+|\xi|^2)^\sigma \mathrm{d}\xi$$

$$\leq \int_{\mathbb{R}^d} (\rho(D)+\varepsilon)^2 |\hat{F}(\xi)|^2_D (1+|\xi|^2)^\sigma \mathrm{d}\xi$$

$$\leq \delta^2 \|F\|^2_{(H^\sigma)^s,D}.$$

This proves (2.13). ∎

Remark 2.5. Let us define $\|\cdot\|_{(H^\sigma)^s,\infty}$ the norm on $(H^\sigma)^s$ defined as the maximum of the H^σ-norm of the components of the vectors. One can check easily that

$$\forall F \in (H^\sigma)^s, \qquad \|F\|_{(H^\sigma)^s,\infty} \leq \|F\|_{(H^\sigma)^s} \leq \sqrt{s}\|F\|_{(H^\sigma)^s,\infty}.$$

In particular, this norm is also equivalent to the norm $\|\cdot\|_{(H^\sigma)^s,D}$.

3. Convergence for linearly implicit methods for NLS and NLH

In this section, we first introduce the consistency and convergence errors of the linearly implicit method (2.2)–(2.5)–(2.7) in Section 3.1. Then, we focus on the anlysis of the quasi-Runge–Kutta step (2.5) in Section 3.2. In Section 3.3, we set the precise hypotheses on the exact solution of (1.1) as well as on the linearly implicit method and we state the main result of the paper, which ensures that linearly implicit methods have high order. The proof of this main result is provided in Section 3.4.

In this section, we assume $\Omega = \mathbb{R}^d$ or $\Omega = \mathbb{T}^d$ even if the results extend to more complex geometries (see Section 2.2).

3.1. Consistency and convergence errors

3.1.1. *Consistency errors*

We assume that the equation (1.1) with initial datum $u^0 \in H^\sigma$ at $t=0$ has a unique smooth solution at least on some interval of the form $(T_\star, T^\star)$ with $T_\star < 0 < T^\star$. We estimate consistency errors. Since consistency errors rely on Taylor expansions of the exact solution with respect to time, the analysis is very similar to that of [21]. For all integer n greater or equal to -1, we denote by t_n the time nh, where $h > 0$ is the time step that we assume sufficiently small to ensure that $T_\star < t_{-1}$.

Definition 3.1. For all $n \geq 0$ and all $h > 0$ small enough such that $t_{n+1} < T^\star$, we define the consistency error R_n^1 in $(H^\sigma)^s$ of the step (2.2) by setting

$$R_n^1 = \begin{bmatrix} N(u(t_n + c_1 h)) \\ \vdots \\ N(u(t_n + c_s h)) \end{bmatrix} - D \begin{bmatrix} N(u(t_{n-1} + c_1 h)) \\ \vdots \\ N(u(t_{n-1} + c_s h)) \end{bmatrix} - N(u(t_n)) \begin{bmatrix} \theta_1 \\ \vdots \\ \theta_s \end{bmatrix}. \tag{3.1}$$

Similarly, we define the consistency error R_n^2 of step (2.4) as the vector of $(H^\sigma)^s$ with entry number i equal to

$$\left(R_n^2\right)_i = u(t_n + c_i h) - u(t_n) - h\sum_{j=1}^{s} a_{ij}\left(L + N(u(t_n + c_j h))\right) u(t_n + c_j h). \tag{3.2}$$

Moreover, we define the consistency error R_n^3 in H^σ of step (2.6) by setting

$$R_n^3 = u(t_{n+1}) - u(t_n) - h \sum_{i=1}^{s} b_i \left(L + N(u(t_n + c_i h))\right) u(t_n + c_i h). \tag{3.3}$$

We fix some final time $T \in (0, T^\star)$.

Proposition 3.2 (consistency error of step (2.2)). *Assume that the exact solution and the nonlinear term are such that $t \longmapsto N \circ u(t)$ has s continuous derivatives in H^σ on $[0, T]$. Assume moreover that the step (2.2) is consistent of order s. There exists a constant $C > 0$ such that for all $n \in \mathbb{N}$ and $h > 0$ sufficiently small, such that $t_{n+1} \leq T$, one has*

$$\|R_n^1\|_{(H^\sigma)^s} \leq C h^s. \tag{3.4}$$

Proof. The proof follows the very same lines as that of Lemma 2.8 in [21]. In particular, Equation (2.3) is crucial in the computation of Taylor expansions. ∎

Proposition 3.3 (consistency error of steps (2.5)–(2.7)). *Assume that the Runge–Kutta method defined in Section 2.1.1 is a collocation method of order s. Assume that the exact solution and the nonlinear term are such that $t \longmapsto u(t)$ has $s + 2$ continuous derivatives in H^σ on $[0, T]$. There exists a constant $C > 0$ such that for all $n \in \mathbb{N}$ and $h > 0$ sufficiently small, such that $t_{n+1} \leq T$, one has*

$$\|R_n^2\|_{(H^\sigma)^s} \leq C h^{s+1} \qquad and \qquad \|R_n^3\|_{H^\sigma} \leq C h^{s+1}. \tag{3.5}$$

Proof. For all $n \geq 0$ and $h > 0$ such that $t_{n+1} \leq T$, the errors $((R_n^2)_i)_{1 \leq i \leq s}$ and (R_n^3) are that of the quadrature method (corresponding to the Runge–Kutta collocation method) applied to the function u' at points $(t_n + c_j h)_{1 \leq j \leq s}$ with weights $(h a_{i,j})_{1 \leq j \leq s}$ on $[t_n, t_n + c_i h]$ for $(R_n^2)_i$ for all $i \in \{1, \ldots, s\}$ and with weights $(h b_i)_{1 \leq i \leq s}$ on $[t_n, t_{n+1}]$ for R_n^3. Therefore, they can be expressed, for example, with the Peano Kernel. They depend on the method, and on the exact solution, but not on the numerical solution. So, since the function $u' \in \mathcal{C}^{s+1}([0, T], H^\sigma)$, they are controlled as in (3.5). ∎

3.1.2. *Convergence errors*

We introduce the notation for the convergence errors that we use in the proof of convergence. Following the notation in the paper [21], we denote for all $h > 0$ small enough to ensure that the method (2.2)–(2.4)–(2.6) is well-defined, and all $n \geq 0$ such that $t_{n+1} \leq T$ the following convergence errors: $P_n \in (H^\sigma)^s$ is the vector with component number i equal to $(P_n)_i = N(u(t_n + c_i h)) - \gamma_{n,i}$, $Q_n \in (H^\sigma)^s$ is the vector with component number i equal to $(Q_n)_i = u(t_n + c_i h) - u_{n,i}$, and $e_n \in H^\sigma$ is defined by $u(t_n) - u_n$. Moreover, we set $z_n = \max_{0 \leq k \leq n}(\|e_k\|_{H^\sigma})$.

3.2. **Analysis of the linear quasi-Runge–Kutta step (2.4)**

3.2.1. *Notions of stability for Runge–Kutta methods*

We denote by $\mathbb{C}^-$ the set of complex numbers with non positive real part, and by $i\mathbb{R}$ the set of purely imaginary numbers. Following [11, 16, 22, 25], we recall the following definitions, using the linear stability function R defined in (2.1).

Definition 3.4. A Runge–Kutta method is said to be

- *A*-stable if for all $\lambda \in \mathbb{C}^-$, $|R(\lambda)| \leq 1$.

- *I*-stable if for all $\lambda \in i\mathbb{R}$, $|R(\lambda)| \leq 1$.

- *AS-stable* if the rational function $\lambda \mapsto \lambda b^t (I - \lambda A)^{-1}$ has only removable singularities in $\mathbb{C}^-$ and is bounded on $\mathbb{C}^-$.

- *ASI*-stable if for all $\lambda \in \mathbb{C}^-$, the matrix $(I - \lambda A)$ is invertible and $\lambda \mapsto (I - \lambda A)^{-1}$ is uniformly bounded on $\mathbb{C}^-$.

- *IS-stable* if the rational function $\lambda \mapsto \lambda b^t (I - \lambda A)^{-1}$ has only removable singularities in $i\mathbb{R}$ and is bounded on $i\mathbb{R}$.

- *ISI*-stable if for all $\lambda \in i\mathbb{R}$, the matrix $(I - \lambda A)$ is invertible and $\lambda \mapsto (I - \lambda A)^{-1}$ is uniformly bounded on $i\mathbb{R}$.

- $\hat{A}$-stable if it is *A*-stable, *AS*-stable and *ASI*-stable.

- $\hat{I}$-stable if it is *I*-stable, *IS*-stable and *ISI*-stable.

A few examples of Runge–Kutta methods and their stability properties can be found in Section 7.3. The analysis of the stability properties of these methods as well as other examples can be found in [22].

Remark 3.5. Observe that, from this definition, an *A*-stable Runge–Kutta collocation method is also *I*-stable. Similarly, an *AS*-stable Runge–Kutta collocation method is also *IS*-stable, and *ASI*-stable Runge–Kutta collocation method is also *ISI*-stable. As a consequence, an $\hat{A}$-stable method is also $\hat{I}$-stable.

Remark 3.6. If b is in the range of A^t, then *ASI*-stability implies *AS*-stability using Lemma 4.4 of [11]. Similarly, *ISI*-stability implies *IS*-stability under the same hypothesis.

Remark 3.7. Further connections between these eight notions of stability for collocation Runge–Kutta methods are analysed in [22].

Remark 3.8. The well posedness of the *linear* PDE (1.1) (with $N \equiv 0$) relies on the fact that the spectrum of the linear operator L is included in a half-plane of the form $\{z \in \mathbb{C} \mid \Re(z) \leq s_0\}$ for some s_0 in $\mathbb{R}$. Up to a change of unknown, we may consider the case $s_0 = 0$ without loss of generality. The first example $L = \Delta$ (see Section 1) fits this framework. The analysis of our methods applied to this example will involve the notion of $\hat{A}$-stability even in the nonlinear setting. Similarly, the second example $L = i\Delta$ (see Section 1) also fits this framework. The analysis of our methods applied to this example will involve the notion of $\hat{I}$-stability even in the nonlinear setting.

3.2.2. *Stability of Runge–Kutta methods for semilinear PDE problems*

In this paper, we consider semilinear evolution problems of the form (1.1), with $L = \Delta$ or $L = i\Delta$ as explained in Section 2.2. What follows can be adapted for any diagonalizable operator on H^σ, provided one knows the localization of the spectrum. The goal of this section is to set notations on the operators that will be used later in the paper and to establish estimates on these operators, provided that the Runge–Kutta method has some stability property. The proof of these estimates is presented in Appendix (Section 7.1).

Proposition 3.9. *Assume that either the Runge–Kutta method is AS-stable and $L = \Delta$ or that the Runge–Kutta method is IS-stable and $L = i\Delta$. There exists a constant $C > 0$ such that for all $h > 0$, we have*

$$\left\| \left(hb^t \otimes L \right) (I - hA \otimes L)^{-1} \right\|_{(H^\sigma)^s \to H^\sigma} \leq C.$$

Proposition 3.10. *Assume that either the Runge–Kutta method is ASI-stable and $L = \Delta$ or that the Runge–Kutta method is ISI-stable and $L = i\Delta$. There exists a constant $C > 0$ such that for all $h > 0$, we have*

$$\| (I - hA \otimes L)^{-1} \|_{(H^\sigma)^s \to (H^\sigma)^s} \le C.$$

3.2.3. *Well-posedness of the quasi-Runge–Kutta step*

Proposition 3.11. *If the chosen Runge–Kutta method is ASI-stable and $L = \Delta$ or if it is ISI-stable and $L = i\Delta$, then the internal linear step (2.5) of the linearly implicit method (2.2)–(2.5)–(2.7) is well defined for $h > 0$ sufficiently small, where "sufficiently small" depends only on the norm of Γ_n in $(H^\sigma)^s$.*

Proof. Assume the method is ISI-stable and $L = i\Delta$ (the proof follows the very same lines in the other case). Since the method is ISI-sable and $L = i\Delta$, Proposition 3.10 ensures that for all $h > 0$, the operator $(I - hA \otimes L)$ has bounded inverse from $(H^\sigma)^s$ to itself, and its operator norm is bounded by a constant that does not depend on h. Solving (2.5) in $(H^\sigma)^s$ is indeed equivalent to solving for U_n in $(H^\sigma)^s$

$$\left(I - h \left(I - hA \otimes L \right)^{-1} A\Gamma_n \bullet \right) U_n = \left(I - hA \otimes L \right)^{-1} u_n \mathbb{1}.$$

Since the operator norm of $(I - hA \otimes L)^{-1} A\Gamma_n \bullet$ is bounded by the product of the operator norm of $(I - hA \otimes L)^{-1}$ by that of $U \mapsto A\Gamma_n \bullet U$, and since the latter only depends on a bound on Γ_n, the result follows using a Neumann series argument. ∎

3.3. **Hypotheses and main result**

With the hypotheses on the exact solution and on T introduced in Section 3.1.1, we choose some $r > 0$ and we denote by V an r-neighbourhood of the exact solution of (1.1) defined by

$$V = \{u(t) + v \mid t \in [0, T] \text{ and } v \in H^\sigma \text{ with } \|v\|_{H^\sigma} \le r\}. \tag{3.6}$$

We make the following hypotheses on the nonlinearity N in (1.1) and on the exact solution of the Cauchy problem.

Hypothesis 3.1. *The function N sends bounded sets of H^σ to bounded sets of H^σ.*

Hypothesis 3.2. *The function N is Lipschitz continuous on bounded sets of H^σ.*

Hypothesis 3.3. *The exact solution u has $s+2$ continuous derivatives with values in H^σ on $(T_\star, T^\star)$.*

Hypothesis 3.4. *The function $t \mapsto N(u(t))$ has s continuous derivatives in H^σ on $(T_\star, T^\star)$.*

We make the following assuptions on the numerical method (2.2)–(2.4)–(2.6).

Hypothesis 3.5. *The Runge–Kutta method is a collocation method with s distinct points $0 \le c_1 < \cdots < c_s \le 1$ (see Definition 2.2).*

Hypothesis 3.6. *The matrix $D \in \mathcal{M}_s(\mathbb{C})$ and the vector $\Theta \in \mathbb{C}^s$ are such that the step (2.2) is strongly stable and consistent of order s. We denote by δ a fixed number in $(\rho(D), 1)$, and by $\| \cdot \|_{(H^\sigma)^s, D}$ the norm on $(H^\sigma)^s$ provided by Lemma 2.4.*

Using Hypothesis 3.4, we have that $N \circ u([0, T])$ is a bounded set of H^σ and we denote by $M > 0$ a bound on this set. Moreover, with Hypothesis 3.1, the set $N(V)$ is bounded and we denote by $m > 0$ a constant such that

$$\forall v \in V, \qquad \|N(v)\|_{H^\sigma} < M + m. \tag{3.7}$$

Let us recall that we chose $\sigma > d/2$ so that H^σ is an algebra (see Section 2.2).

Theorem 3.12. *Assume that the function N in (1.1) satisfies Hypotheses 3.1 and 3.2. Assume $u^0 \in H^\sigma$ is fixed and that $T \in (0, T^\star)$, $r > 0$ and V are defined as in (3.6). Assume the exact solution satisfies Hypotheses 3.3 and 3.4. Assume $M > 0$ and $m > 0$ are defined as in (3.7).*

Assume that the underlying Runge–Kutta method satisfies Hypothesis 3.5 and that the step (2.2) satisfies Hypothesis 3.6. Assume that the underlying Runge–Kutta method is $\hat{I}$-stable and $L = i\Delta$, or that the underlying Runge–Kutta method is $\hat{A}$-stable and $L = \Delta$.

There exists a constant $C \geq 1$, a small $h_0 \in (0, T)$ and a neighbourhood of $u^0 \in H^\sigma$ such that for all u_0 in this neighbourhood, all $h \in (0, h_0)$ and all $\gamma_{-1,1}, \ldots, \gamma_{-1,s}$ sufficiently close their continuous analogues $N(u(t_{-1} + c_1 h)), \ldots, N(u(t_{-1} + c_s h))$, the numerical method (2.2), (2.4), (2.6) is well defined for all $n \in \mathbb{N}$ such that $0 \leq nh \leq T$. Moreover, for such n and h, the method satisfies

$$\forall i \in \{1, \ldots, s\}, \qquad \|\gamma_{n-1,i}\|_{H^\sigma} \leq M + m, \tag{3.8}$$

and

$$\max_{0 \leq k \leq n} \|u(t_k) - u_k\|_{H^\sigma} \leq e^{Cnh} \left(\left\|u^0 - u_0\right\|_{H^\sigma} + C \left(\max_{i \in \{1, \ldots, s\}} \|N(u(t_{-1} + c_i h)) - \gamma_{-1,i}\|_{H^\sigma} + h^s \right) \right). \tag{3.9}$$

3.4. **Proof of Theorem 3.12**

We recall that the consistency errors have been defined in Section 3.1.1 and the convergence errors have been defined in Section 3.1.2. In the following proof, the letter C denotes a real number greater or equal to 1, which does not depend on h (but depends on M and r in particular) and whose value may vary from one line to the other.

Using Hypothesis 3.6, step (2.2) is strongly stable. Therefore, we fix $\delta \in (\rho(D), 1)$ and we use Lemma 2.4 to define a norm $\| \cdot \|_{(H^\sigma)^s, D}$ such that (2.13) holds.

We divide the proof in two parts. First, we assume an a priori bound for the numerical solution. Assume we are given an integer $\nu \in \mathbb{N}$ such that $t_{\nu+1} \leq T$ and for all $n \leq \nu$,

(H1) $\|\Gamma_n\|_{(H^\sigma)^s, \infty} \leq M + m$,

(H2) the step (2.4) has a unique solution $(u_{n,i})_{1 \leq i \leq s}$ in $(H^\sigma)^s$,

(H3) $u_n \in V$.

We show that, in this case, we have an explicit bound for the convergence errors $(P_n)_{0 \leq n \leq \nu}$ and $(z_n)_{0 \leq n \leq \nu}$ (see equations (3.21) and (3.23)).

Second, we assume that h_0 and the initial errors P_{-1} and e_0 are small enough and we show that the bounds of the first part of the proof are indeed satisfied.

First part. In addition to the bounds above, we assume that $h \in (0, 1)$. Let us consider $n \in \mathbb{N}$ with $n \leq \nu$. In particular, we have $t_{n+1} \leq T$. Substracting (2.2) from (3.1) we obtain

$$P_n = DP_{n-1} + (N(u(t_n)) - N(u_n)) \begin{bmatrix} \theta_1 \\ \vdots \\ \theta_s \end{bmatrix} + R_n^1. \tag{3.10}$$

We infer using estimate (2.13) of Lemma 2.4

$$\|P_n\|_{(H^\sigma)^s, D} \leq \delta \|P_{n-1}\|_{(H^\sigma)^s, D} + C\|e_n\|_{H^\sigma} + \|R_n^1\|_{(H^\sigma)^s, D}, \tag{3.11}$$

where the constant C is proportional to the Lipschitz constant of N over the bounded set V (using Hypothesis 3.2).

Substracting (2.4) from (3.2) we obtain

$$Q_{n,i} = e_n + h \sum_{j=1}^{s} a_{i,j} \left(L Q_{n,j} + N(u(t_n + c_j h)) u(t_n + c_j h) - \gamma_{n,j} u_{n,j} \right) + (R_n^2)_i$$

$$= e_n + h \sum_{j=1}^{s} a_{i,j} L Q_{n,j} + h \sum_{j=1}^{s} a_{i,j} \left(N(u(t_n + c_j h)) - \gamma_{n,j} \right) u(t_n + c_j h)$$

$$+ h \sum_{j=1}^{s} a_{i,j} \gamma_{n,j} \left(u(t_n + c_j h) - u_{n,j} \right) + (R_n^2)_i$$

$$= e_n + h \sum_{j=1}^{s} a_{i,j} L Q_{n,j} + h \sum_{j=1}^{s} a_{i,j} P_{n,j} u(t_n + c_j h) + h \sum_{j=1}^{s} a_{i,j} \gamma_{n,j} Q_{n,j} + (R_n^2)_i.$$

Therefore, the vector Q_n solves

$$(I - hA \otimes L) Q_n = e_n \mathbb{1} + hA P_n \bullet U_{t_n} + hA \Gamma_n \bullet Q_n + R_n^2, \tag{3.12}$$

where U_{t_n} is the vector with component j equal to $u(t_n + c_j h)$. Since the Runge–Kutta method is either $\hat{I}$-stable or $\hat{A}$-stable, it is either ISI-stable or ASI-stable and the operator $I - hA \otimes L$ is invertible (see Proposition 3.10) and the equation above is equivalent to

$$(I - h(I - hA \otimes L)^{-1} A \Gamma_n \bullet) Q_n = (I - hA \otimes L)^{-1} \left(e_n \mathbb{1} + hA P_n \bullet U_{t_n} + R_n^2 \right).$$

Just as in Proposition 3.11 the operator in the left hand side is invertible for h small depending only on a bound on $\|\Gamma_n\|_{(H^\sigma)^s, \infty}$. Let us denote by $\|\cdot\|_\star$ the operator norm in $((H^\sigma)^s, \|\cdot\|_{(H^\sigma)^s, \infty})$. As soon as $h\|(I - hA \otimes L)^{-1} A \Gamma_n \bullet\|_\star < 1$, we have

$$\|Q_n\|_{(H^\sigma)^s, \infty} \leq C \frac{1}{1 - h\|(I - hA \otimes L)^{-1} A \Gamma_n \bullet\|_\star} \left(\|e_n\|_{H^\sigma} + Ch\|P_n\|_{(H^\sigma)^s, \infty} + \|R_n^2\|_{(H^\sigma)^s, \infty} \right).$$

Note that, using (H1), $\|A \Gamma_n \bullet\|_\star \leq C_1(M + m)$, where C_1 only depends on the matrix A. Since $\|(I - hA \otimes L)^{-1}\|_{(H^\sigma)^s \to (H^\sigma)^s}$ is bounded by a constant that does not depend on h, the same holds for $\|(I - hA \otimes L)^{-1}\|_\star$ with a constant C_2. Then, provided that h is sufficiently small to ensure that $h C_1 C_2 (M + m) \leq 1/2$, we have, increasing C again if necessary,

$$\|Q_n\|_{(H^\sigma)^s, \infty} \leq C \|e_n\|_{H^\sigma} + Ch\|P_n\|_{(H^\sigma)^s, \infty} + C\|R_n^2\|_{(H^\sigma)^s, \infty}. \tag{3.13}$$

Substracting (2.6) from (3.3) we obtain

$$e_{n+1} = e_n + h \sum_{i=1}^{s} b_i L Q_{n,i} + h \sum_{i=1}^{s} b_i \left(N(u(t_n + c_i h)) - \gamma_{n,i} \right) u(t_n + c_i h)$$

$$+ h \sum_{i=1}^{s} b_i \gamma_{n,i} \left(u(t_n + c_i h) - u_{n,i} \right) + R_n^3$$

$$= e_n + h \sum_{i=1}^{s} b_i L Q_{n,i} + h \sum_{i=1}^{s} b_i P_{n,i} u(t_n + c_i h) + h \sum_{i=1}^{s} b_i \gamma_{n,i} Q_{n,i} + R_n^3$$

$$= e_n + h(b^t \otimes L) Q_n + hb^t(P_n \bullet U_{t_n}) + hb^t(\Gamma_n \bullet Q_n) + R_n^3$$

$$= e_n + h(b^t \otimes L)(I - hA \otimes L)^{-1} e_n \mathbb{1}$$

$$+ h(b^t \otimes L)(I - hA \otimes L)^{-1} \left[hA P_n \bullet U_{t_n} + hA \Gamma_n \bullet Q_n + R_n^2 \right]$$

$$+ hb^t P_n \bullet U_{t_n} + hb^t \Gamma_n \bullet Q_n + R_n^3, \tag{3.14}$$

where we have used (3.12).

Let us denote by $v_n = e_n + h(b^t \otimes L)(I - hA \otimes L)^{-1} e_n \mathbb{1}$. Assume that the spatial domain is $\Omega = \mathbb{R}^d$. Observe that if $L = i\Delta$, then for all $\xi \in \mathbb{R}^d$,

$$\widehat{v_n}(\xi) = R(-ih\xi^2)\widehat{e_n}(\xi),$$

and that if $L = \Delta$, then for all $\xi \in \mathbb{R}^d$,

$$\widehat{v_n}(\xi) = R(-h\xi^2)\widehat{e_n}(\xi),$$

where R is the linear stability function of the Runge–Kutta method defined in (2.1). Since the Runge–Kutta method is either $\hat{I}$-stable or $\hat{A}$-stable, it is either I-stable or A-stable and in both cases, hence $|R| \le 1$ in the appropriate region. Similar estimates hold in the periodic case $\Omega = \mathbb{T}^d$. Therefore,

$$\|v_n\|_{H^\sigma} \le \|e_n\|_{H^\sigma}.$$

Since the Runge–Kutta method is either $\hat{I}$-stable or $\hat{A}$-stable, it is either IS-stable or AS-stable and in both cases, using (3.14), we infer with Proposition 3.9, that

$$\|e_{n+1}\|_{H^\sigma} \le \|e_n\|_{H^\sigma} + Ch\|P_n\|_{(H^\sigma)^s,\infty} + Ch\|\Gamma_n\|_{(H^\sigma)^s,\infty}\|Q_n\|_{(H^\sigma)^s,\infty} + C\|R_n^2\|_{(H^\sigma)^s} + \|R_n^3\|_{H^\sigma},$$

which gives with (H1)

$$\|e_{n+1}\|_{H^\sigma} \le \|e_n\|_{H^\sigma} + Ch\|P_n\|_{(H^\sigma)^s,\infty} + Ch(M+m)\|Q_n\|_{(H^\sigma)^s,\infty} + C\|R_n^2\|_{(H^\sigma)^s} + \|R_n^3\|_{H^\sigma}.$$

Using (3.13), and recalling that $h \in (0,1)$ so that $h^2 \le h \le 1$, we have

$$\|e_{n+1}\|_{H^\sigma} \le (1+Ch)\|e_n\|_{H^\sigma} + Ch\|P_n\|_{(H^\sigma)^s,\infty} + C\|R_n^2\|_{(H^\sigma)^s} + \|R_n^3\|_{H^\sigma}. \tag{3.15}$$

From (3.11) we have by induction

$$\|P_n\|_{(H^\sigma)^s,D} \le \delta^{n+1}\|P_{-1}\|_{(H^\sigma)^s,D} + C\sum_{k=0}^{n} \delta^{n-k}\left(\|e_k\|_{H^\sigma} + \|R_k^1\|_{(H^\sigma)^s,D}\right). \tag{3.16}$$

Using the norm equivalence between $\|\cdot\|_{(H^\sigma)^s,\infty}$ and $\|\cdot\|_{(H^\sigma)^s,D}$, and (3.16) in (3.15) we obtain

$$\|e_{n+1}\|_{H^\sigma} \le (1+Ch)\|e_n\|_{H^\sigma} + Ch\left[\delta^{n+1}\|P_{-1}\|_{(H^\sigma)^s,D} + C\sum_{k=0}^{n}\delta^{n-k}\left(\|e_k\|_{H^\sigma} + \|R_k^1\|_{(H^\sigma)^s,D}\right)\right]$$
$$+ C\|R_n^2\|_{(H^\sigma)^s} + \|R_n^3\|_{H^\sigma}. \tag{3.17}$$

With estimate (3.5), we infer that

$$\|e_{n+1}\|_{H^\sigma} \le (1+Ch)\|e_n\|_{H^\sigma} + Ch\left[\delta^{n+1}\|P_{-1}\|_{(H^\sigma)^s,D} + C\sum_{k=0}^{n}\delta^{n-k}\left(\|e_k\|_{H^\sigma} + \|R_k^1\|_{(H^\sigma)^s,D}\right)\right]$$
$$+ Ch^{s+1}. \tag{3.18}$$

Using the maximal error defined previously and the fact that $\delta < 1$ since the step (2.2) is strongly stable, we have, using also estimate (3.4),

$$\|e_{n+1}\|_{H^\sigma} \le (1+Ch)z_n + Ch\left[\delta^{n+1}\|P_{-1}\|_{(H^\sigma)^s,D} + (z_n + h^s)\sum_{k=0}^{n}\delta^{n-k}\right] + Ch^{s+1}$$
$$\le (1+Ch)z_n + Ch\left[\delta^{n+1}\|P_{-1}\|_{(H^\sigma)^s,D} + (z_n + h^s)\frac{1}{1-\delta}\right] + Ch^{s+1},$$

and then

$$\|e_{n+1}\|_{H^\sigma} \le (1+Ch)z_n + Ch\delta^{n+1}\|P_{-1}\|_{(H^\sigma)^s,D} + Ch^{s+1}. \tag{3.19}$$

Using that $z_{n+1} = \max\{z_n, \|e_{n+1}\|_{H^\sigma}\}$, we infer

$$z_{n+1} \le (1+Ch)z_n + Ch\|P_{-1}\|_{(H^\sigma)^s,D} + Ch^{s+1}. \tag{3.20}$$

By induction it follows that for all n in $\mathbb{N}$ such that $t_n \leq T$,

$$
\begin{aligned}
z_n &\leq (1 + Ch)^n z_0 + Ch \left(\|P_{-1}\|_{(H^\sigma)^s, D} + h^s \right) \sum_{k=0}^{n-1} (1 + Ch)^k \\
&\leq e^{Cnh} z_0 + Ch \left(\|P_{-1}\|_{(H^\sigma)^s, D} + h^s \right) \frac{(1 + Ch)^n}{1 + Ch - 1} \\
&\leq e^{Cnh} \left(z_0 + C \left(\|P_{-1}\|_{(H^\sigma)^s, D} + h^s \right) \right) \\
&\leq e^{Cnh} \left(z_0 + C \left(\|P_{-1}\|_{(H^\sigma)^s, \infty} + h^s \right) \right).
\end{aligned}
\tag{3.21}
$$

Using (3.16) and the same estimations as above, we have moreover, since $\delta < 1$,

$$
\|P_n\|_{(H^\sigma)^s, D} \leq \|P_{-1}\|_{(H^\sigma)^s, D} + C(z_n + h^s).
\tag{3.22}
$$

We infer, using (3.21),

$$
\|P_n\|_{(H^\sigma)^s, \infty} \leq C e^{Cnh} \left(z_0 + \|P_{-1}\|_{(H^\sigma)^s, \infty} + h^s \right).
\tag{3.23}
$$

This shows that, as long as (H1), (H2) and (H3) hold for n such that $0 \leq n \leq \nu$, the estimates (3.21) and (3.23)) hold for the convergence errors $(P_n)_{0 \leq n \leq \nu}$ and $(z_n)_{0 \leq n \leq \nu}$. Observe that the constant $C > 1$ above does not depend on h, neither does it depend on ν. However, it depends on the exact solution through the hypotheses stated before the theorem. This concludes the first part of the proof.

Second part. From now on, we denote by C the maximum of the constants appearing in the right hand sides of (3.21) and (3.23). Choose $h_0 \in (0, 1)$ sufficiently small to have $h_0 < \min\{-T_\star, T^\star\}$ and $C e^{CT} h_0^s < r$ and $C e^{CT} h_0^s < m$ and $h_0 C_1 C_2 (M + m) \leq 1/2$ where C_1 and C_2 were defined in the first part. Assume $u_0, \gamma_{-1+c_1}, \ldots, \gamma_{-1+c_s} \in H^\sigma$ and $h \in (0, h_0)$ satisfy

$$
e^{CT} \left(\|u^0 - u_0\|_{H^\sigma} + C \left(\max_{i \in [\![1, s]\!]} \|\gamma_{-1+c_i} - N(u(t_{-1} + c_i h))\|_{H^\sigma} + h_0^s \right) \right) < r,
\tag{3.24}
$$

and

$$
C e^{CT} \left(\|u^0 - u_0\|_{H^\sigma} + \max_{i \in [\![1, s]\!]} \|\gamma_{-1+c_i} - N(u(t_{-1} + c_i h))\|_{H^\sigma} + h_0^s \right) < m.
\tag{3.25}
$$

First, with (3.23) (for $n = 0$) and (3.25), we have

$$
\|P_0\|_{(H^\sigma)^s, \infty} = \max_{i \in [\![1, s]\!]} \|\gamma_{0+c_i} - N(u(t_0 + c_i h))\|_{H^\sigma} < m.
$$

Therefore by triangle inequality we have

$$
\|\Gamma_0\|_{(H^\sigma)^s, \infty} \leq \|P_0\|_{(H^\sigma)^s, \infty} + \|(N(u(t_0 + c_i h)))_{1 \leq i \leq s}\|_{(H^\sigma)^s, \infty} < M + m.
$$

And then, the hypothesis (H1) of the first part is satisfied for $n = 0$.

Moreover, with (3.24), we have $\|u^0 - u_0\|_{H^\sigma} \leq r$ so that $u_0 \in V$ and the hypothesis (H3) of the first part is satisfied with $n = 0$. With Proposition 3.11, we infer that the system (2.5) has a unique solution in $(H^\sigma)^s$ since we assumed $h \leq h_0 < 1/(2C_1 C_2 (M + m))$. This implies that the hypothesis (H2) of the first part is satisfied for $n = 0$. Then we can apply the analysis of the first part (with $\nu = 0$) to obtain (3.21) and (3.23) with $n = 1$. Using (3.24) and (3.25), we infer that hypotheses (H1), (H2) and (H3) are satisfied for all $n \leq \nu = 1$, and the result follows by induction on ν.

4. **Remark on the mass conservation for NLS equation**

Let us consider the NLS equation (1.1) with $L = i\Delta$ and N taking values in $i\mathbb{R}$, such that the Cauchy problem associated to (1.1) is well-posed. In this case, the L^2-norm of the solution is preserved by the exact flow (at least in the case $\Omega = \mathbb{R}^d$ and $\Omega = \mathbb{T}^d$). Indeed, classically, one has along the exact solution u:

$$\frac{1}{2}\frac{\mathrm{d}}{\mathrm{d}t}\|u(t)\|^2 = \Re\left(\int_\Omega \left(-i|\nabla u|^2 + N(u)|u|^2\right)\mathrm{d}x\mathrm{d}y\right) = 0.$$

For linearly implicit methods, it is possible to reproduce this property numerically, by adapting a classical condition for the preservation of quadratic invariants by Runge–Kutta methods [26].

Proposition 4.1. *Assume $L = i\Delta$ and N takes values in $i\mathbb{R}$. Assume the collocation Runge–Kutta method satisfies the Cooper condition*

$$\forall 1 \leq i, j \leq s, \qquad b_i b_j - b_i a_{ij} - b_j a_{ji} = 0. \tag{4.1}$$

Assume the eigenvalues of D are chosen so that D is a real valued squared matrix and θ is a real valued vector. If $\gamma_{-1,1}, \ldots, \gamma_{-1,s}$ take values in $i\mathbb{R}$, then for all $u_0 \in L^2(\Omega)$ and for all $n \in \mathbb{N}$ such that u_n is well-defined by the linearly implicit method, one has

$$\|u_n\|^2 = \|u_0\|^2.$$

Proof. Let n be given as in the hypothesis. We have, using (2.6):

$$\int_\Omega |u_{n+1}|^2 = \int_\Omega u_{n+1}\overline{u_{n+1}}$$

$$= \int_\Omega \left[\left(u_n + h\sum_{i=1}^s b_i(L + \gamma_{n+c_i})u_{n,i}\right)\overline{\left(u_n + h\sum_{i=1}^s b_i(L + \gamma_{n+c_i})u_{n,i}\right)}\right]$$

$$= \int_\Omega |u_n|^2 + h\int_\Omega I_1 + h\int_\Omega I_2 + h^2\int_\Omega I_3, \tag{4.2}$$

where, since $b_i \in \mathbb{R}$,

$$I_1 = \sum_{i=1}^s b_i\overline{(L + \gamma_{n+c_i})u_{n,i}}\ u_n,$$

$$I_2 = \sum_{i=1}^s b_i(L + \gamma_{n+c_i})u_{n,i}\overline{u_n},$$

$$I_3 = \sum_{i,j=1}^s b_i b_j(L + \gamma_{n+c_i})u_{n,i}\overline{(L + \gamma_{n+c_j})u_{n,j}}.$$

Using (2.4), we can write:

$$I_1 = \sum_{i=1}^s b_i\left(\overline{(L + \gamma_{n+c_i})}\overline{u_{n,i}}\right)u_{n,i} - h\sum_{i=1}^s b_i\left(\overline{(L + \gamma_{n+c_i})}\overline{u_{n,i}}\right)\left(\sum_{j=1}^s a_{i,j}(L + \gamma_{n+c_j})u_{n,j}\right),$$

$$= \sum_{i=1}^s b_i\left(\overline{(L + \gamma_{n+c_i})}\overline{u_{n,i}}\right)u_{n,i} - h\sum_{j=1}^s b_j\left(\overline{(L + \gamma_{n+c_j})}\overline{u_{n,j}}\right)\left(\sum_{i=1}^s a_{j,i}(L + \gamma_{n+c_i})u_{n,i}\right),$$

$$= \sum_{i=1}^s b_i\left(\overline{(L + \gamma_{n+c_i})}\overline{u_{n,i}}\right)u_{n,i} - h\sum_{j=1}^s\left(\sum_{i=1}^s b_j a_{j,i}(L + \gamma_{n+c_i})u_{n,i}\overline{(L + \gamma_{n+c_j})}\overline{u_{n,j}}\right).$$

A similar computation leads to

$$I_2 = \sum_{i=1}^s b_i\left((L + \gamma_{n+c_i})u_{n,i}\right)\overline{u_{n,i}} - h\sum_{j=1}^s\left(\sum_{i=1}^s b_i a_{i,j}(L + \gamma_{n+c_i})u_{n,i}\overline{(L + \gamma_{n+c_j})}\overline{u_{n,j}}\right).$$

339

Using these two equalities in (4.2), we obtain

$$\int_\Omega |u_{n+1}|^2 = \int_\Omega |u_n|^2 + h \sum_{i=1}^{s} b_i \int_\Omega \left[\overline{(L + \gamma_{n+c_i})u_{n,i}}\, u_{n,i} + (L + \gamma_{n+c_i})u_{n,i}\overline{u_{n,i}} \right]$$

$$+ h^2 \sum_{j=1}^{s} \sum_{i=1}^{s} (b_i b_j - b_i a_{i,j} - b_j a_{j,i}) \int_\Omega (L + \gamma_{n+c_i})u_{n,i}\overline{(L + \gamma_{n+c_j})u_{n,j}}.$$

With the Cooper condition (4.1) in the last term, this gives

$$\int_\Omega |u_{n+1}|^2 = \int_\Omega |u_n|^2 + 2h \sum_{i=1}^{s} b_i \operatorname{Re}\left(\int_\Omega (L + \gamma_{n+c_i})u_{n,i}\overline{u_{n,i}} \right). \tag{4.3}$$

Observe that, since the $(\gamma_{-1+c_i})_{1\leq i \leq s}$ are purely imaginary-valued initially, D is a real-valued matrix, and N takes values in $i\mathbb{R}$, the step (2.2) ensures by induction that $(\gamma_{n+c_i})_{1\leq i \leq s}$ are purely imaginary-valued. Using that and the fact that, for the Schrödinger equation, the operator $L = i\Delta$ is skew-symmetric, we infer that the last term in (4.3) is equal to zero. This implies

$$\int_\Omega |u_{n+1}|^2 = \int_\Omega |u_n|^2.$$

This concludes the proof. ∎

5. Numerical experiments

This section is devoted to numerical experiments illustrating the main theorem of the paper (Theorem 3.12). We also demonstrate numerically the necessity of the stability conditions of Section 3.2 for the convergence result to hold. Moreover, we compare the precision and efficiency of the linearly implicit methods analysed in this paper with that of classical methods from the literature. We consider NLS equations in 1D (Section 5.2) and 2D (Section 5.3), as well as NLH equations in 1D (Section 5.4). A more extensive numerical comparison of linearly implicit methods for several semilinear evolution PDEs will be the object of a forthcoming paper.

5.1. Note on the initialization of the linearly implicit methods

Initializing a linearly implicit method (2.2), (2.4), (2.6) requires not only an approximation u_0 of u^0 but also s approximations $\gamma_{-1,1}, \ldots, \gamma_{-1,s}$ of $N(u(t_{-1+c_1})), \ldots, N(u(t_{-1+c_s}))$. To do so, in the numerical experiments below, we use appropriate methods that ensure that the corresponding terms in the right hand-side of (3.9) has order s. This is easy to do for NLS equations since they are reversible with respect to time. For non reversible equations like NLH equations, we may compute forward approximations of $N(u(t_{0+c_1})), \ldots, N(u(t_{0+c_s}))$ and $u(t_1)$, by standard methods of sufficient orders and use these values as initial data for the linearly implicit method after a shift of h in time.

5.2. Numerical experiments in 1 dimension for the NLS equation

We perform numerical experiments in dimension 1 ($\Omega = \mathbb{R}$), on the soliton solution

$$u(t,x) = \sqrt{\frac{2\alpha}{q}} \operatorname{sech}\left(\sqrt{\alpha}(x - x_0 - ct)\right) e^{i(\alpha + \frac{c^2}{4})t} e^{ic(x - x_0 - ct)/2}, \tag{5.1}$$

to the NLS equation (1.1) with $L = i\partial_x^2$ and $N(u) = iq|u|^2$ for some $q \in \mathbb{R} \setminus \{0\}$, x_0 real, c real, $\alpha > 0$.

We initialize the methods by a projection of this exact solution on the space grid for u^0 and by the image by N of the projection of this exact solution on the space grid for $\gamma_{-1,1}, \ldots, \gamma_{-1,s}$. The final error is computed comparing to the projection on the space grid of the exact solution at final time.

5.2.1. *Methods of order 2*

The linearly implicit method with the underlying Runge–Kutta method of Example 7.4 and $\pm \frac{1}{2}$ as eignevalues of D, applied to a nonlinear Schrödinger equation with exact solution (5.1) with $q = 4$, $\alpha = 1$, $c = 0$ and $x_0 = 0$, has been implemented in [21]. The computational domain was truncated to $(-50, 50)$ with homogeneous Dirichlet boundary conditions and discretized with 2^{18} points in space. The final computational time was $T = 5$. Observe that this method is $\hat{A}$-stable (see Example 7.4).

We refer the reader to Figure 4 in [21] for the numerical comparison with other convergent methods of order 2 from the literature (the Crank–Nicolson method and the Strang splitting method). The left panel shows the order 2 of each method and in particular illustrates Theorem 3.12 for the linearly implicit method. Moreover, the right panel shows the efficiency of the methods in terms of CPU time as a function of the error: The numerical cost for a given error is a bit higher for the linearly implicit method of order 2 than for the Strang splitting method and it is much lower than for the Crank–Nicolson method.

To complete the illustration of Theorem 3.12 for methods of order 2, we investigate the relevance of the hypothesis of $\hat{A}$-stability for the underlying Runge–Kutta method. To this end, we implement the linearly implicit method relying on the Runge–Kutta method described in Example 7.5 with $\pm \frac{1}{2}$ as eigenvalues of D on the same soliton test case. This underlying Runge–Kutta method is not A-stable (and even not I-stable) and hence not $\hat{A}$-stable. We emphasize the fact that this linearly implicit method is of order 2 when applied to an ODE thanks to Theorem 9 in [21]. However, Figure 5.1 shows that this method fails to converge for the soliton case. This demonstrates the relevance of the hypothesis of A-stability (or at least I-stability) for the numerical solution of nonlinear Schrödinger equations using linearly implicit methods (this is in fact similar to the use of classical Runge–Kutta methods for the numerical solution of semi-discretized linear or nonlinear Schrödinger equations, where A-stability (or at least I-stability) is required as well to ensure convergence).
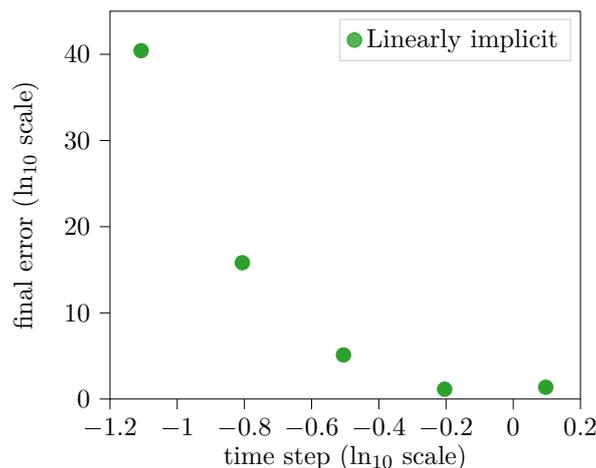

FIGURE 5.1. Numerical error as a function of the time step for the soliton test case with the linearly implicit method based on the Runge–Kutta collocation method of Example 7.5 which is not $\hat{A}$-stable (since not A-stable) with $\lambda_1 = 1/2, \lambda_2 = -1/2$.

Moreover, these examples illustrate that, even if the eigenvalues of the matrix D are chosen inside the open unit disc, in order to ensure that the step (2.2) is strongly stable in the sense of Definition 2.1, a linearly implicit method may fail to be convergent for stability reasons (in the last example : because the underlying collocation Runge–Kutta method is not $\hat{A}$-stable).

5.2.2. *Methods of order 4*

For the numerical methods of order 4, we use the parameters $q = 8$, $x_0 = 0$, $c = 0.5$, $\alpha = 4$ in the nonlinear Schrödinger equation and its exact solution (5.1) above. The computational domain is truncated to $(-62.5; 62.5)$ and we set homogeneous Dirichlet boundary conditions. We use finite differences with 2^{20} points in space for each method. We denote by $\mathcal{L}$ the classical homogeneous Dirichlet Laplacian matrix times the purely imaginary unit. We perform the simulation until $T = 5$.
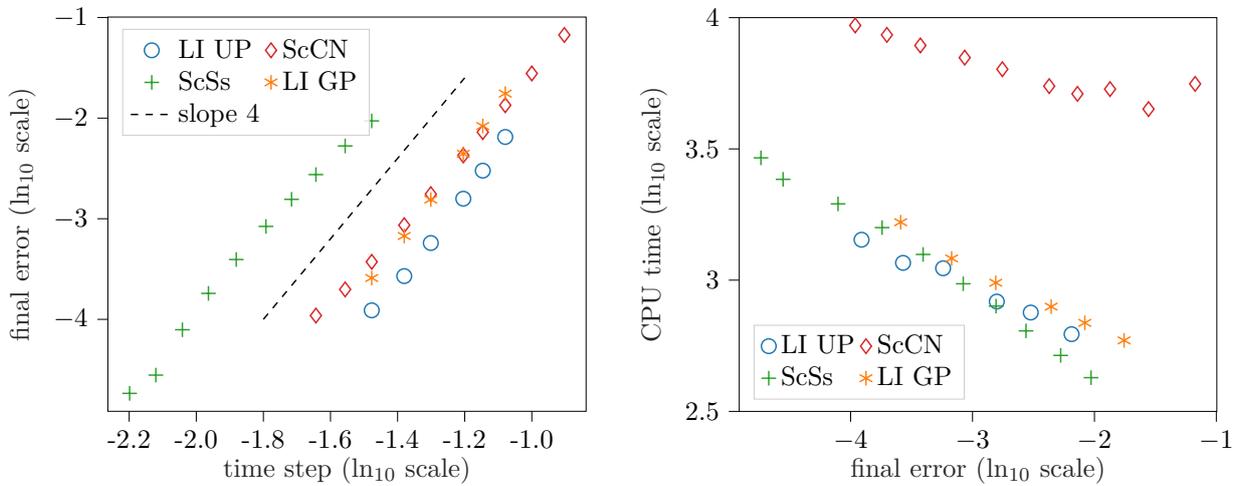

FIGURE 5.2. Comparison of methods of order 4 applied to the NLS equation. On the left panel, maximal numerical error as a function of the time step (logarithmic scales); on the right panel, CPU time (in seconds) as a function of the final numerical error (logarithmic scales).

We compare four numerical methods of order 4 on the 1D soliton case mentioned above :

- the linearly implicit method of order 4 (LI UP) defined by $(c_1, c_2, c_3, c_4) = (0, \frac{1}{3}, \frac{2}{3}, 1)$ and $(\lambda_1, \lambda_2, \lambda_3, \lambda_4) = (\frac{i}{2}, -\frac{i}{2}, \frac{i}{4}, -\frac{i}{4})$. The corresponding coefficients $(a_{i,j})_{1 \leq i,j \leq 4}$ and $(b_i)_{1, \leq i \leq 4}$ are computed in Example 7.6. The underlying Runge–Kutta method is $\hat{A}$-stable.

- the linearly implicit method of order 4 (LI GP) with Gauss points defined by

$$(c_1, c_2, c_3, c_4) = \left(\frac{1}{2} - \frac{\alpha_1}{70}, \frac{1}{2} - \frac{\alpha_2}{70}, \frac{1}{2} + \frac{\alpha_2}{70}, \frac{1}{2} + \frac{\alpha_1}{70} \right),$$

where $\alpha_1 = \sqrt{525 + 70\sqrt{30}}$ and $\alpha_2 = \sqrt{525 - 70\sqrt{30}}$ and $\lambda_1 = -1/4$, $\lambda_2 = 1/4$, $\lambda_3 = -1/2$, $\lambda_4 = 1/2$. The underlying Runge–Kutta method is $\hat{A}$-stable (see [22]).

- the Suzuki composition (see (5.4)) of the Crank–Nicolson method (ScCN) where the Crank–Nicolson method $\Phi_h : u_n \mapsto u_{n+1}$ is given by:

$$\frac{u_{n+1} - u_n}{h} = \left(\mathcal{L} + \frac{N(u_{n+1}) + N(u_n)}{2} \right) \frac{u_{n+1} + u_n}{2}, \tag{5.2}$$

- the Suzuki composition (see (5.4)) of the Strang splitting method (ScSs) where the Strang splitting method $\Phi_h : u_n \mapsto u_{n+1}$ is given by:

$$
\begin{cases}
u_{n,1} = \exp\left(hN(u_n)/2\right) u_n, \\
\left(1 - \dfrac{h}{2}\mathcal{L}\right) u_{n,2} = \left(1 + \dfrac{h}{2}\mathcal{L}\right) u_{n,1}, \\
u_{n+1} = \exp\left(hN(u_{n,2})/2\right) u_{n,2}.
\end{cases}
\tag{5.3}
$$

The Suzuki composition method that we use is given by the following numerical flow:

$$
\Phi_{\alpha_3 h} \circ \Phi_{\alpha_2 h} \circ \Phi_{\alpha_1 h},
\tag{5.4}
$$

with $\alpha_1 = \alpha_3 = \frac{1}{2 - \sqrt[3]{2}}$ and $\alpha_2 = 1 - 2\alpha_1$. Since the methods Φ_h are symmetric and of order 2, their composition (5.4) above is symmetric of order 4.

The results of Figure 5.2 indicate that the four methods above have order 4 in this soliton case (left panel). This illustrates Theorem 3.12 for the linearly implicit methods. Moreover, the two linearly implicit methods of order 4 outperform the ScCN method in terms of efficiency (computational time required for a given error) and so does the ScSs method (right panel). Indeed, the two linearly implicit methods and ScSs, as implemented above, require to solve a linear system at each time step and they display similar efficiencies within the final error range used for this simulation.

5.2.3. *A method of order 5*

For the illustration of the importance of the *ASI*-stability of the underlying collocation Runge–Kutta method hypothesis, we implement the 5-stages linearly implicit method defined in Example 7.7. For that linearly implicit method the underlying Runge–Kutta method is *A*-stable, *AS*-stable, but not *ASI*-stable. We use it to solve numerically the nonlocal nonlinear evolution PDE

$$
\partial_t u = i\partial_x^2 u + u \star u \star u,
\tag{5.5}
$$

with periodic boundary conditions on the torus $\mathbb{R}/(2\pi\mathbb{Z})$ and where $\star$ denotes the convolution product. To understand the Cauchy theory for equation (5.5), note that the evolution of the Fourier coefficient $c_k(u)$ of order $k \in \mathbb{Z}$ is such that

$$
(c_k(u(t, \cdot))^2 = \frac{(c_k(u_0))^2}{\left(1 - i\frac{(c_k(u_0))^2}{k^2}\right) e^{2ik^2 t} + i\frac{(c_k(u_0))^2}{k^2}},
\tag{5.6}
$$

where u_0 is the initial datum associated to (5.5) at $t = 0$. Assuming that $u_0 \in L^2(\mathbb{R}/(2\pi\mathbb{Z}))$ is real-valued and even, we have that for all $k \in \mathbb{Z}$, $c_k(u_0) \in \mathbb{R}$ and taking appropriate square roots in (5.6), and forming the corresponding Fourier series, we obtain a solution to (5.5) for all $t \in \mathbb{R}$. We plot in Figure 5.3 the discrete L^2-norm of the difference at times close to $T = 1.0$ between the exact solution of (5.5) defined using (5.6) and the numerical solution obtained by the non-ASI method described in Example 7.7. We take $N = 30$ Fourier modes (from $k = 0$ to $k = 29$) and $c_k(u_0) = e^{-|k|}$. We chose time steps between $1.0/2^3$ and $1.0/2^8$ and we also consider time steps satisfying $1 - hk^2\alpha = 0$, where $\alpha = 3\sqrt{7}/56$ (see the analysis of this method carried out in [22]). For these time steps, the matrix $(I - hA \otimes L)$ (for diagonal L with entries $-ik^2$) is not invertible. We observe in Figure 5.3 that the method displays a convergence of order 5 for regular time steps, which is destroyed for resonant time steps of the form $1.0/(\alpha k^2)$. This illustrates the importance of the hypothesis of *ASI*-stability (included in $\hat{A}$-stability) in Theorem 3.12 for the convergence of linearly implicit methods applied to a nonlinear Schrödinger evolution PDE.

Remark 5.1. The numerical examples above (in Figure 5.1 of a method which is not *A*-stable (see Section 5.2.1) and in Figure 5.3 of a method which is *A*, *AS* and not *ASI* stable (see Section 5.2.3)),
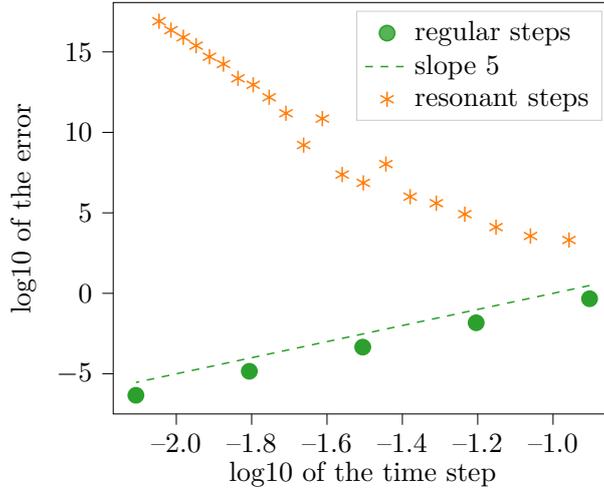
FIGURE 5.3. Numerical L^2-error at time $T = 1.0$ as a function of the time step for the solution to Equation (5.5) with initial datum given in the text through its Fourier coefficients, using the non-ASI linearly implicit method of order 5 described in Example 7.7. We plot regular time steps of the form $1.0/2^p$ for $p \in \{3, \dots, 8\}$ (green dots), a regular line of slope 5 (dashed green line), and resonant time steps of size $1.0/(\alpha k^2)$ for $1 \le k \le 30$.

show that linearly implicit methods may fail to converge for evolution PDE problems, even if they would converge for evolution ODE problems. Moreover, these two numerical examples demonstrate the relevance of the concepts of A-stability and ASI-stability in the hypotheses of Theorem 3.12.

5.3. **Numerical experiments in 2 dimensions for the NLS equation**

5.3.1. *Space discretization*

We consider the focusing NLS equation

$$i\partial_t u = -\Delta u - q|u|^2 u, \tag{5.7}$$

on a star-shaped domain $\mathcal{S} \subset \mathbb{R}^2$ with homogeneous Dirichlet boundary conditions, with $q \in \mathbb{R}$. The energy associated to (5.7) reads

$$E(u) = \frac{1}{2} \int_{\mathcal{S}} |\nabla u|^2 \mathrm{d}x\mathrm{d}y - \frac{q}{4} \int_{\mathcal{S}} |u|^4 \mathrm{d}x\mathrm{d}y.$$

The domain $\mathcal{S}$ consists in the union of the interior of the triangle with vertices

$$\left(R\sin\left(2k\frac{\pi}{3}\right), R\cos\left(2k\frac{\pi}{3}\right) \right), \qquad 0 \le k \le 2,$$

and that of the triangle with vertices

$$\left(R\sin\left((2k+1)\frac{\pi}{3}\right), R\cos\left((2k+1)\frac{\pi}{3}\right) \right), \qquad 0 \le k \le 2,$$

for some $R > 0$.

The discretization of $\mathcal{S}$ is carried out using `GMSH` by generating an admissible (in the sense of finite volumes) triangular mesh of $\mathcal{S}$. The triangles are denoted $(\mathcal{T}_j)_{1 \le j \le J}$ for some $J \ge 1$. The set of the corresponding edges is denoted by $\mathcal{E}$, and is partitioned in the set $\mathcal{E}^{\text{int}}$ of interior edges (belonging to 2 triangles) and the set $\mathcal{E}^{\text{ext}}$ of exterior edges (belonging to 1 triangle). For all triangle $\mathcal{T}_j$, we denote by

$\mathcal{E}_j \subset \mathcal{E}$ the set of its 3 edges. Denoting by $U \in \mathbb{C}^J$ a finite volume approximation of a complex-valued function u over $\mathcal{S}$, we define a $J \times J$ matrix L by setting for all $k \in \{1, \ldots, J\}$

$$(LU)_k = \frac{i}{m\left(\mathcal{T}_k\right)} \left(\sum_{\sigma \in \mathcal{E}_k \cap \mathcal{E}^{\text{int}}} \frac{U_j - U_k}{d_\sigma} \ell_\sigma + \sum_{\sigma \in \mathcal{E}_k \cap \mathcal{E}^{\text{ext}}} \frac{0 - U_k}{d_\sigma} \ell_\sigma \right),$$

where

- in the first sum, for $\sigma \in \mathcal{E}_k \cap \mathcal{E}^{\text{int}}$, the letter j denotes *the* integer in $\{1, \ldots, J\} \setminus \{k\}$ such that σ is both an edge of $\mathcal{T}_j$ and $\mathcal{T}_k$, d_σ is the distance between the centers of mass of $\mathcal{T}_j$ and $\mathcal{T}_k$ and ℓ_σ is the length of the edge σ;

- in the second sum, for $\sigma \in \mathcal{E}_k \cap \mathcal{E}^{\text{ext}}$, d_σ denotes the distance between the center of mass of $\mathcal{T}_k$ and the edge σ, and ℓ_σ still denotes the length of the edge σ;

- the area of the triangle $\mathcal{T}_k$ is denoted by $m\left(\mathcal{T}_k\right)$. In our case all the triangles share the same area $m(\mathcal{T})$.

This way, LU is a finite volume approximation of $i\Delta u$. It is easy to check that the matrix L is skew-symmetric, with spectrum included in $i\mathbb{R}^-$. From now on, we consider the following semidiscretization of (5.7):

$$U'(t) = LU(t) + N(U) * U, \tag{5.8}$$

where $N(U) \in \mathbb{R}^J$ has component j equal to $iq|U_j|^2$ and $*$ stands for the componentwise multiplication in $\mathbb{C}^J$.

5.3.2. *Comparison of methods of order 2 on the star shaped domain*

We consider the case $q = 1$, $R = 1$ with the initial datum U_0 as the interpolation of

$$u_0(x, y) = \sqrt{\frac{98}{\pi}} \exp\left(-49(x^2 + y^2)\right) \exp\left(-20ix\right),$$

at the centers of the triangles. We set $T = 0.1$ as the final time. An example of the dynamics is presented in Figure 5.4 with $J = 161472$ triangles.

Note that, since the spectrum of L is not explicitly known, the computation of exponentials involving L requires approximations. Depending on where these approximations are used (in splitting methods, in e.g. Lawson methods, or in exponential Runge–Kutta methods), the order of approximation has to be chosen carefully. Moreover, when J is big, computing these approximations can be costly.

We present in Figure 5.5 a numerical comparison with $J = 10\,092$ of methods expected to be of order 2 for this problem. We show at the same time the final error as a function of the time step (left panel) and the CPU time as a function of the final error (right panel), both in log scales. The four methods we consider are

- the Strang splitting method with $(\text{Id} + hL/2)(\text{Id} - hL/2)^{-1}$ as an approximation of e^{hL} in a classical and efficient implementation involving only the Lie splitting method,

- the Crank–Nicolson method (C-N),

- the linearly implicit method with uniform points (LI UP) based on the Runge–Kutta method of Example 7.4 with $\lambda_1 = -\lambda_2 = 1/2$,

- the linearly implicit method with Gauss points (LI GP) based on the Runge–Kutta method of Example 7.3 with $\lambda_1 = -\lambda_2 = 1/2$.
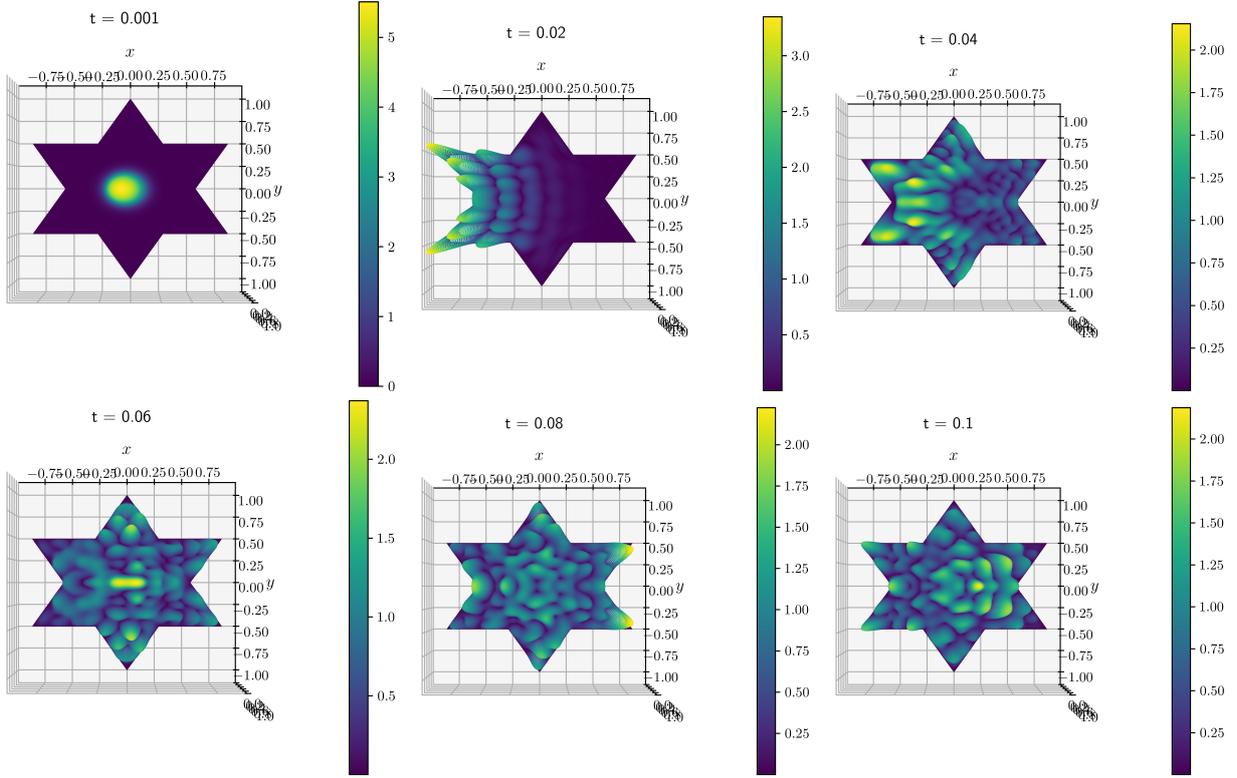
FIGURE 5.4. The dynamics of the test case of the NLS equation (5.7) on a star-shaped domain.

We implement the four methods in `Python` and use the `spsolve` function of `sparse.linalg` of `scipy` to compute the solutions to all the linear systems. We use a reference solution computed with a method of order 5 with a very small time step to compute the final errors. The three first methods have numerical order 2 as predicted by Theorem 3.12. The fourth one seems to have order 3 and hence to behave even better than predicted by Theorem 3.12. In terms of efficiency, the linearly implicit method with Gauss points outperforms even the explicit Strang splitting method described above. However, the Strang splitting method is faster than the linearly implicit method with uniform points.

We compare in Figure 5.6 the preservation property of the mass (squared L^2-norm) and energy

$$E(U) = \frac{m(\mathcal{T})}{2} U^\star L U - q \frac{m(\mathcal{T})}{4} \sum_{k=1}^{J} |U_k|^4, \tag{5.9}$$

where $U^\star$ is the conjugate transpose of U. As expected, the Crank–Nicolson method and Strang splitting method preserve the mass. So does the linearly implicit method with Gauss points since it satisfies the Cooper condition (4.1). This is coherent with Proposition 4.1. The linearly implicit method with uniform points does not preserve mass as it does not satisfy the Cooper condition. Among the four methods of order 2, the Crank–Nicolson method is the only one preserving the energy.

5.4. **Numerical experiments in 1 dimension for the NLH equation**

The comparaison of methods of order 1 has been carried out in [21]. We focus here on methods of order 2.
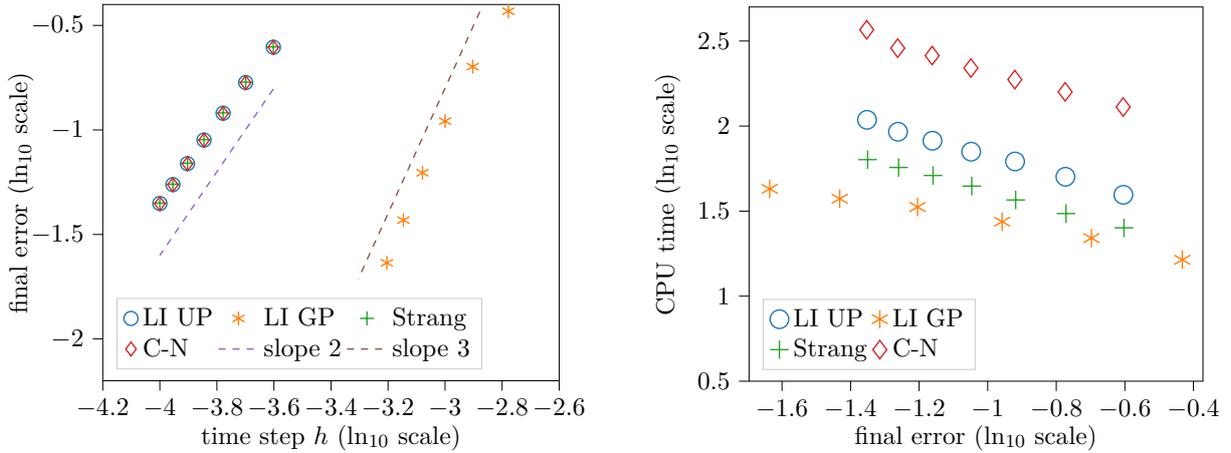
FIGURE 5.5. Comparison for $J = 10\,092$ of methods of order 2 applied to the NLS equation on a star-shaped domain. On the left panel, final numerical error as a function of the time step (logarithmic scales); on the right panel, CPU time (in seconds) as a function of the final numerical error (logarithmic scales).
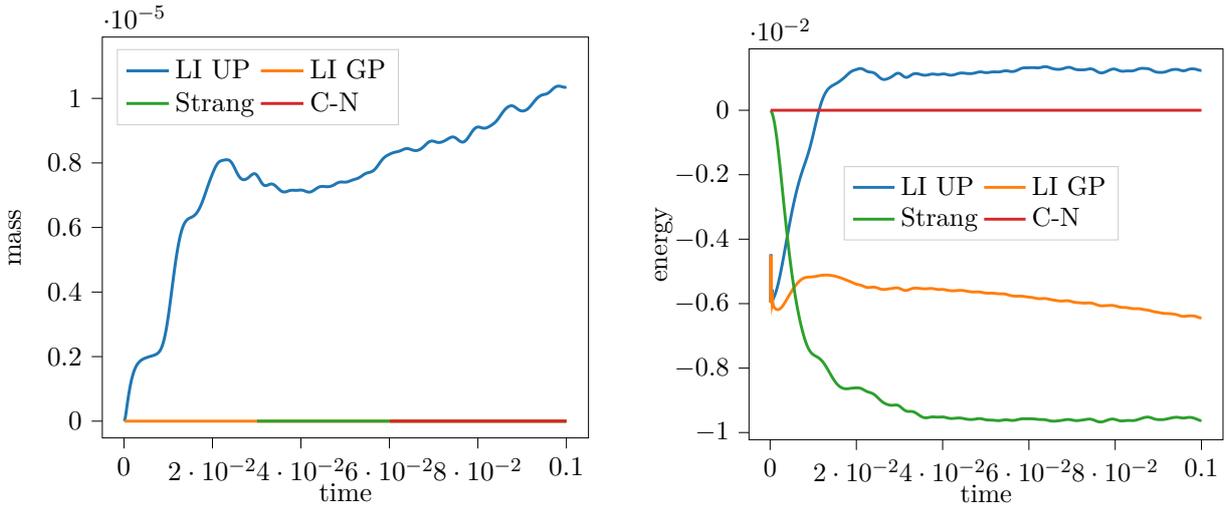

FIGURE 5.6. Deviation of the mass (left panel) and energy (right panel) from their initial values by the four methods of order 2 for $J = 10\,092$ and $h = 10^{-4}$

In this section, we perform numerical experiments in dimension 1 on $\Omega = (-50, 50)$ with homogeneous Dirichlet boundary conditions, on the equation

$$\partial_t u(t, x) = \partial_{xx}^2 u(t, x) + u(t, x)^3, \tag{5.10}$$

starting from

$$u_0(x) = \frac{1}{2} \sin\left(\frac{\pi}{100} x + \frac{\pi}{2}\right),$$

for $t \in (0, T)$ with $T = 1.0$. We use classical finite differences in space with 2^{14} points. We compare two linearly implicit methods (with uniform (Example 7.4) or Gauss points (Example 7.3), the eigenvalues of the matrix D being $\pm\frac{1}{2}$ in both cases) with the classical methods of Crank–Nicolson (see (5.2) for that method for the NLS equation) and Strang splitting (see (5.3) for that method for the NLS

equation). A reference solution is computed with a classical Runge–Kutta method of order 10 with a small time step. For the initialization of the linearly implicit methods, we use one step of Strang splitting starting from u_0 over $[0, c_1 h]$, $[0, c_2 h]$ and $[0, h]$ and then run the method (see Section 5.1). Numerical results are displayed in Figure 5.7.
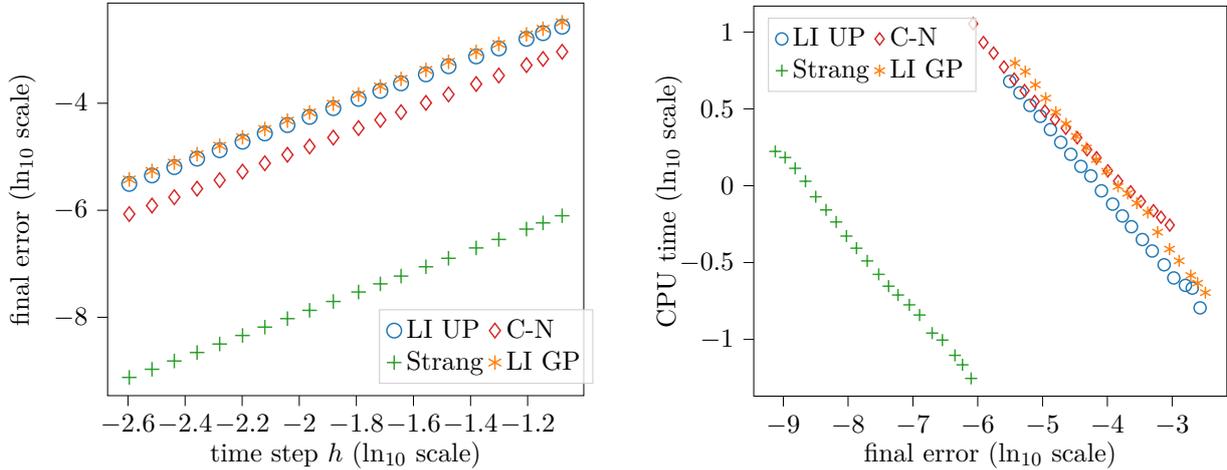

FIGURE 5.7. Comparison for 2^{14} points of methods of order 2 applied to the NLH equation (5.10) over $(-50, 50)$ with Dirichlet boundary conditions. On the left panel, final numerical error as a function of the time step (logarithmic scales); on the right panel, CPU time (in seconds) as a function of the final numerical error (logarithmic scales).

The underlying Runge–Kutta methods of both linearly implicit methods are $\hat{A}$-stable and the eignevalues of their matrix D belong to the open unit disc. Therefore, Theorem 3.12 ensures that they converge with order (at least) 2. The numerical experiment described above demonstrates numerically that both methods have order 2. For this numerical example, the Strang splitting appears to be the most precise and the most efficient of all four methods. The two linearly implicit methods have an efficiency which is comparable to that of the Crank–Nicolson method.

6. **Conclusion and future works**

This paper extends the analysis of high order linearly implicit methods developped for ODEs in [21] to the numerical integration of evolution semilinear PDEs. It introduces several notions of stability for the underlying collocation Runge–Kutta method, the analysis of which is carried out in the companion paper [22]. Assuming these stability conditions as well as additional stability conditions for the extra variables, the main result of this paper states that linearly implicit method with s stages have order at least s (Theorem 3.12).

The necessity of all the stability conditions is illustrated numerically. Numerical experiments for the NLS and NLH equations illustrate the efficiency of the linearly implicit methods in dimensions 1 and 2 when compared with classical methods from the literature. In particular one obtains better performance for high order linearly implicit methods in dimension 2.

More extensive numerical experiments will be carried out in a forthcoming paper.

7. Appendix

7.1. Proof of Proposition 3.10

This section is devoted to the proof of the estimates of Propositions 3.9, and 3.10. For the sake of brevity, we only write the proof of Proposition 3.10 in the case of the torus in the case of ASI-stability and $L = \Delta$. The proof of the other cases can be derived using the same technique: the case of *ISI*-stability with $L = i\Delta$ is the very same, with a different localization of the spectrum of L, and that of 3.9 has to be adapted for isomophisms that are not endomorphisms. That technique has to be adapted for other continuous cases, for example when $L = \Delta$ or $L = i\Delta$ on $\mathbb{R}^d$, but the spirit is the same.

Proof. Let us consider the case of the torus $\Omega = (\mathbb{R}/\mathbb{Z})^d$, with the Laplace operator $L = \Delta$. Let $\sigma > 0$ and $h > 0$ be fixed. Since L is an unbounded operator from H^σ to itself, with domain $H^{\sigma+2}$, and is selfadjoint over H^σ, we have

$$H^\sigma = \overline{\bigoplus_{\lambda \in \mathrm{Sp}(L)} \mathrm{Ker}(L - \lambda \, \mathrm{Id}_{H^\sigma})}.$$

Defining for $\lambda \in \mathrm{Sp}(L)$, V_λ as $(\mathrm{Ker}(L - \lambda \, \mathrm{Id}_{H^\sigma}))^s$, we infer

$$(H^\sigma)^s = \overline{\bigoplus_{\lambda \in \mathrm{Sp}(L)} V_\lambda}. \tag{7.1}$$

Observe that, for all $\lambda \in \mathrm{Sp}(L)$, V_λ is stable by $A \otimes L$. Moreover, for all $\lambda \in \mathrm{Sp}(L)$ and $(v_1, \ldots, v_s) \in V_\lambda$, we have

$$(A \otimes L) \begin{pmatrix} v_1 \\ \vdots \\ v_s \end{pmatrix} = \lambda A \begin{pmatrix} v_1 \\ \vdots \\ v_s \end{pmatrix}. \tag{7.2}$$

Observe that $\mathrm{Sp}(L) \subset (-\infty, 0]$. Let $\lambda \in \mathrm{Sp}(L)$ be fixed. We have $h\lambda \in \mathbb{C}^-$. In particular, with the hypothesis that the method defining A is *ASI*-stable (see Definition 3.4), the matrix $(I - h\lambda A)$ is invertible. This, together with (7.2), implies that $(\mathrm{Id}_{(H^\sigma)^s} - hA \otimes L)_{|V_\lambda}$ is invertible from V_λ to itself. Moreover, using the norm defined in (2.12), we have

$$\left\| \left[\left(\mathrm{Id}_{(H^\sigma)^s} - hA \otimes L \right)_{|V_\lambda} \right]^{-1} \right\|_{(H^\sigma)^s \to (H^\sigma)^s} = \left\| (I - h\lambda A)^{-1} \right\|_2,$$

where the norm in the right-hand side is the usual hermitian norm on $\mathbb{C}^s$. Since this holds for all $\lambda \in \mathrm{Sp}(L)$ and the spaces V_λ are pairwise orthogonal, we can use (7.1) to derive that $(\mathrm{Id}_{(H^\sigma)^s} - h\lambda A \otimes L)$ is invertible from $(H^\sigma)^s$ to itself, with

$$\left\| \left(\mathrm{Id}_{(H^\sigma)^s} - hA \otimes L \right)^{-1} \right\|_{(H^\sigma)^s \to (H^\sigma)^s} \leq \sup_{\lambda \in \mathrm{Sp}(L)} \left\| (I - h\lambda A)^{-1} \right\|_2.$$

The hypothesis that the method defining A is ASI-stable ensures that the right-hand side of the inequality above is bounded independantly of $h > 0$. This concludes the proof. ∎

7.2. Two technical lemmas

Lemma 7.1. *Let $D \in \mathcal{M}_s(\mathbb{C})$. We denote by $\rho(D)$ the spectral radius of the matrix D and by $|\cdot|_2$ the usual hermitian norm on $\mathbb{C}^s$. For all $\varepsilon > 0$, there exists an invertible matrix P such that*

$$\forall x \in \mathbb{C}^s, \qquad |PDP^{-1}x|_2 \leq (\rho(D) + \varepsilon) |x|_2. \tag{7.3}$$

Proof. Let D and ε as in the hypotheses. Using for example the Jordan reduction theorem for the matrix D, there exists an invertible matrix $U \in \mathcal{M}_s(\mathbb{C})$ such that UDU^{-1} is upper triangular. The coefficients on the diagonal of UDU^{-1} are therefore the complex eigenvalues $\lambda_1, \dots, \lambda_s$ of D. After conjugation by the diagonal matrix M_δ with diagonal elements $1, \delta, \dots, \delta^{s-1}$ for $\delta \in (0,1)$, we obtain

$$M_\delta U D (M_\delta U)^{-1} = \begin{pmatrix} \lambda_1 & \delta t_{1,2} & \delta^2 t_{1,3} & \dots & \delta^{s-1} t_{1,s} \\ 0 & \lambda_2 & \delta t_{2,1} & \dots & \delta^{s-2} t_{2,s} \\ \vdots & \ddots & \ddots & \ddots & \vdots \\ 0 & & \ddots & \lambda_{s-1} & \delta t_{s-1,s} \\ 0 & \dots & \dots & 0 & \lambda_s \end{pmatrix},$$

where the coefficients $(t_{i,j})$ are that of the upper triangular part of UDU^{-1}. For all vector $u \in \mathbb{C}^s$ with $|u|_2 \leq 1$, we infer

$$|M_\delta U D (M_\delta U)^{-1} u|_2^2$$

$$= \sum_{k=1}^s \left| \lambda_k u_k + \delta \sum_{j=k+1}^s \delta^{j-k-1} t_{k,j} u_j \right|^2$$

$$= \sum_{k=1}^s \left[|\lambda_k u_k|^2 + 2\delta \Re \left(\overline{\lambda_k u_k} \sum_{j=k+1}^s \delta^{j-k-1} t_{k,j} u_j \right) + \delta^2 \left| \sum_{j=k+1}^s \delta^{j-k-1} t_{k,j} u_j \right|^2 \right]$$

$$\leq \sum_{k=1}^s \rho(D)^2 |u_k|^2 + 2\delta \sum_{k=1}^s \rho(D) |u|_\infty \sum_{j=k+1}^s \delta^{j-k-1} |t_{k,j}||u_j| + \delta^2 \sum_{k=1}^s \left| \sum_{j=k+1}^s \delta^{j-k-1} |t_{k,j}||u_j| \right|^2$$

$$\leq \rho(D)^2 + 2C\delta\rho(D)s|u|_1 + \delta^2 C^2 s |u|_1^2,$$

where C denotes the maximum of the moduli of the $(t_{i,j})_{i<j}$ and we have used the fact that $|u|_\infty \leq |u|_2 \leq 1$. Since we have $|u|_1 \leq \sqrt{s}|u|_2 \leq \sqrt{s}$, we infer finally that

$$|M_\delta U D (M_\delta U)^{-1} u|_2^2 \leq \rho(D)^2 + 2C s^{3/2} \delta \rho(D) + C^2 \delta^2 s^2.$$

Chosing $\delta \in (0,1)$ small enough to ensure that $\delta \left(2C s^{3/2} \rho(D) + C^2 \delta s^2 \right) \leq \varepsilon^2$, we infer that for all $u \in \mathbb{C}^s$ with $|u|_2 \leq 1$,

$$|M_\delta U D (M_\delta U)^{-1} u|_2 \leq \sqrt{\rho(D)^2 + \varepsilon^2} \leq \rho(D) + \varepsilon.$$

This implies (7.3) with $P = M_\delta U$ by homogeneity. ∎

Lemma 7.2. *Let $D \in \mathcal{M}_s(\mathbb{C})$. We denote by $\rho(D)$ the spectral radius of the matrix D. For all $\varepsilon > 0$, there exists a norm $|\cdot|_D$ on $\mathbb{C}^s$ such that*

$$\forall x \in \mathbb{C}^s, \qquad |Dx|_D \leq (\rho(D) + \varepsilon) \, |x|_D. \tag{7.4}$$

In particular, for the norm $\|\cdot\|_D$ on $\mathcal{M}_s(\mathbb{C})$ induced by $|\cdot|_D$, we have

$$\|D\|_D \leq \rho(D) + \varepsilon.$$

Proof. One obtains the result by setting for all $x \in \mathbb{C}^s$, $|x|_D = |Px|_2$ with the notations of Lemma 7.1. ∎

7.3. **Underlying collocation Runge–Kutta methods used for numerical examples**

This section is devoted to introducing the collocation Runge–Kutta methods used for numerical examples. Details on the stability properties (see Definition 3.4) can be found in [22].

Example 7.3 (Collocation Runge–Kutta method with $s = 2$ Gauss points)**.** For $s = 2$ Gauss points the method reads,

$$\begin{array}{c|cc} \frac{1}{2} - \frac{\sqrt{3}}{6} & \frac{1}{4} & \frac{1}{4} - \frac{\sqrt{3}}{6} \\ \frac{1}{2} + \frac{\sqrt{3}}{6} & \frac{1}{4} + \frac{\sqrt{3}}{6} & 1/4 \\ \hline & \frac{1}{2} & \frac{1}{2} \end{array} , \qquad (7.5)$$

It is $\hat{A}$-stable (see [22]). It is of order 4 ("superconvergence") as a standalone collocation Runge–Kutta method and, when embedded in a linearly implicit method, allows to reach order 2, thanks to Theorem 3.12 (see the method LI GP in Figures 5.5 and 5.7 for example).

Example 7.4 (Trapezoidal rule with $s = 2$ stages)**.** The Runge–Kutta collocation method with $s = 2$ and $(c_1, c_2) = (0, 1)$ reads

$$\begin{array}{c|cc} 0 & 0 & 0 \\ 1 & \frac{1}{2} & \frac{1}{2} \\ \hline & \frac{1}{2} & \frac{1}{2} \end{array} .$$

It is $\hat{A}$-stable (see [22]). It is of order 2 as a standalone collocation Runge–Kutta method and, when embedded in a linearly implicit method, allows to reach order 2, thanks to Theorem 3.12 (see the method LI UP in Figures 5.5 and 5.7 for example).

Example 7.5 (Collocation Runge–Kutta method with $s = 2$ stages not A nor I stable)**.** The Butcher tableau of the Runge–Kutta collocation method with $s = 2$ and $(c_1, c_2) = (1/4, 1/3)$ reads

$$\begin{array}{c|cc} \frac{1}{4} & \frac{5}{8} & -\frac{3}{8} \\ \frac{1}{3} & \frac{2}{3} & -\frac{1}{3} \\ \hline & -2 & 3 \end{array} .$$

It is *neither A*-stable *nor I*-stable (see [22]). It is of order 2 as a standalone collocation Runge–Kutta method and, when embedded in a linearly implicit method, may fail to provide a convergent method for NLS or NLH equations (see Figure 5.1 for example).

Example 7.6 (Lobatto collocation method with $s = 4$ uniform points)**.** The Butcher tableau of the Runge–Kutta collocation method with $s = 4$ and $(c_1, c_2, c_3, c_4) = (0, \frac{1}{3}, \frac{2}{3}, 1)$ reads:

$$\begin{array}{c|cccc} 0 & 0 & 0 & 0 & 0 \\ 1/3 & 1/8 & 19/72 & -5/72 & 1/72 \\ 2/3 & 1/9 & 4/9 & 1/9 & 0 \\ 1 & 1/8 & 3/8 & 3/8 & 1/8 \\ \hline & 1/8 & 3/8 & 3/8 & 1/8 \end{array} .$$

This method is $\hat{A}$-stable (see [22]). It is of order 4 as a standalone collocation Runge–Kutta method and, when embedded in a linearly implicit method, allows to reach order 4, thanks to Theorem 3.12 (see the method LI UP in Figure 5.2 for example).

Example 7.7 (Collocation Runge–Kutta method with $s = 5$ stages which is A, AS but not ASI stable)**.** We consider the 5-stages Runge–Kutta collocation method defined by its Butcher tableau

$$
\begin{array}{c|ccccc}
\frac{1}{4} & \frac{3259}{1440} & -\frac{1421}{720} - \frac{21\sqrt{7}}{64} & \frac{163}{120} & -\frac{1421}{720} + \frac{21\sqrt{7}}{64} & \frac{829}{1440} \\
\frac{1}{2} - \frac{\sqrt{7}}{14} & \frac{\kappa_-^2(281\sqrt{7}+1120)}{15435} & -\frac{343}{180} - \frac{107\sqrt{7}}{315} & \frac{\kappa_-^2(106\sqrt{7}+455)}{10290} & -\frac{\kappa_-^2(97\sqrt{7}+770)}{17640} & \frac{\kappa_-^2(71\sqrt{7}+280)}{15435} \\
\frac{1}{2} & \frac{203}{90} & -\frac{343}{180} - \frac{7\sqrt{7}}{24} & \frac{22}{15} & -\frac{343}{180} + \frac{7\sqrt{7}}{24} & \frac{53}{90} \\
\frac{1}{2} + \frac{\sqrt{7}}{14} & -\frac{\kappa_+^2(281\sqrt{7}-1120)}{15435} & \frac{\kappa_+^2(97\sqrt{7}-770)}{17640} & -\frac{\kappa_+^2(106\sqrt{7}-455)}{10290} & -\frac{343}{180} + \frac{107\sqrt{7}}{315} & -\frac{\kappa_+^2(71\sqrt{7}-280)}{15435} \\
\frac{3}{4} & \frac{363}{160} & -\frac{147}{80} - \frac{21\sqrt{7}}{64} & \frac{63}{40} & -\frac{147}{80} + \frac{21\sqrt{7}}{64} & \frac{93}{160} \\
\hline
 & \frac{128}{45} & \frac{-343}{90} & \frac{44}{15} & \frac{-343}{90} & \frac{128}{45}
\end{array},
$$

where $\kappa_\pm = 7 \pm \sqrt{7}$. This method is A-stable, AS-stable, yet not ASI-stable (see [22]). It is of order 6 as a standalone collocation Runge–Kutta method and, when embedded in a linearly implicit method, it may fail to provide a convergent method for an NLS equation (see Figure 5.3 for example). For the linearly implicit method, we choose $\lambda_i = i/6$ for $i \in \{1, \ldots, 5\}$. Therefore, we have

$$
\Theta = \begin{bmatrix}
\frac{1153}{1944} + \frac{3707\,c_1}{1944} + \frac{3283\,(c_1-1)^2}{7776} + \frac{61\,(c_1-1)^3}{1944} + \frac{5\,(c_1-1)^4}{7776} \\
\frac{1153}{1944} + \frac{3707\,c_2}{1944} + \frac{3283\,(c_2-1)^2}{7776} + \frac{61\,(c_2-1)^3}{1944} + \frac{5\,(c_2-1)^4}{7776} \\
\frac{1153}{1944} + \frac{3707\,c_3}{1944} + \frac{3283\,(c_3-1)^2}{7776} + \frac{61\,(c_3-1)^3}{1944} + \frac{5\,(c_3-1)^4}{7776} \\
\frac{1153}{1944} + \frac{3707\,c_4}{1944} + \frac{3283\,(c_4-1)^2}{7776} + \frac{61\,(c_4-1)^3}{1944} + \frac{5\,(c_4-1)^4}{7776} \\
\frac{1153}{1944} + \frac{3707\,c_5}{1944} + \frac{3283\,(c_5-1)^2}{7776} + \frac{61\,(c_5-1)^3}{1944} + \frac{5\,(c_5-1)^4}{7776}
\end{bmatrix}.
$$

Example 7.8 (Collocation Runge–Kutta with $s = 5$ stages which is I but not A stable)**.** We consider the 5-stages Runge–Kutta collocation method defined by its Butcher tableau

$$
\begin{array}{c|ccccc}
\frac{1}{4} & \frac{4453}{2400} & -\frac{4347}{1600} & \frac{221}{120} & -\frac{1917}{1600} & \frac{1123}{2400} \\
\frac{1}{3} & \frac{3824}{2025} & -\frac{133}{50} & \frac{742}{405} & -\frac{179}{150} & \frac{944}{2025} \\
\frac{1}{2} & \frac{281}{150} & -\frac{513}{200} & \frac{29}{15} & -\frac{243}{200} & \frac{71}{150} \\
\frac{2}{3} & \frac{3808}{2025} & -\frac{194}{75} & \frac{824}{405} & -\frac{28}{25} & \frac{928}{2025} \\
\frac{3}{4} & \frac{1503}{800} & -\frac{4131}{1600} & \frac{81}{40} & -\frac{1701}{1600} & \frac{393}{800} \\
\hline
 & \frac{176}{75} & -\frac{189}{50} & \frac{58}{15} & -\frac{189}{50} & \frac{176}{75}
\end{array}.
$$

This method is I-stable but not A-stable (see [22]). It is of order 6 as a standalone collocation Runge–Kutta method.

References

[1] Georgios Akrivis and Michel Crouzeix. Linearly Implicit Methods for Nonlinear Parabolic Equations. *Math. Comput.*, 73(246):613–635, 2004.

[2] Georgios Akrivis and Vassilios A. Dougalis. On a class of conservative, highly accurate Galerkin methods for the Schrödinger equation. *ESAIM, Math. Model. Numer. Anal.*, 25(6):643–670, 1991.

[3] Georgios Akrivis, Charalambos Makridakis, and Ricardo H. Nochetto. A posteriori error estimates for the Crank–Nicolson method for parabolic equations. *Math. Comput.*, 75(254):511–531, 2006.

[4] Grégoire Allaire and Alan Craig. *Numerical Analysis and Optimization: An Introduction to Mathematical Modelling and Numerical Simulation.* Numerical Mathematics and Scientific Computation. Oxford University Press, 2007.

[5] Nadine Badr, Frédéric Bernicot, and Emmanuel Russ. Algebra properties for Sobolev spaces – Applications to semilinear PDE's on manifolds. *J. Anal. Math.*, 118(2):509–544, 2012.

[6] Christophe Besse. A relaxation scheme for the nonlinear Schrödinger equation. *SIAM J. Numer. Anal.*, 42(3):934–952, 2004.

[7] Christophe Besse, Brigitte Bidégaray, and Stéphane Descombes. Order Estimates in Time of Splitting Methods for the Nonlinear Schrödinger Equation. *SIAM J. Numer. Anal.*, 40(1):26–40, 2002, `https://arxiv.org/abs/https://doi.org/10.1137/S0036142900381497`.

[8] Christophe Besse, Rémi Carles, and Florian Méhats. An asymptotic preserving scheme based on a new formulation for NLS in the semiclassical limit. *Multiscale Model. Simul.*, 11(4):1228–1260, 2013.

[9] Christophe Besse, Stéphane Descombes, Guillaume Dujardin, and Ingrid Lacroix-Violet. Energy-preserving methods for nonlinear Schrödinger equations. *IMA J. Numer. Anal.*, 41(1):618–653, 2020, `https://arxiv.org/abs/https://academic.oup.com/imajna/article-pdf/41/1/618/35971306/drz067.pdf`.

[10] Christophe Besse, Guillaume Dujardin, and Ingrid Lacroix-Violet. High order exponential integrators for nonlinear Schrödinger equations with application to rotating Bose–Einstein condensates. *SIAM J. Numer. Anal.*, 55(3):1387–1411, 2017.

[11] Kevin Burrage, Willem H. Hundsdorfer, and Jan G. Verwer. A study of *B*-convergence of Runge–Kutta methods. *Computing*, 36(1-2):17–34, 1986.

[12] Mari Paz Calvo, Javier de Frutos, and Julia Novo. Linearly implicit Runge–Kutta methods for advection-reaction-diffusion equations. *Appl. Numer. Math.*, 37(4):535–549, 2001.

[13] François Castella, Philippe Chartier, Stéphane Descombes, and Gilles Vilmart. Splitting methods with complex times for parabolic equations. *BIT*, 49:487–508, 2009.

[14] Qing Cheng and Jie Shen. Multiple Scalar Auxiliary Variable (MSAV) Approach and its Application to the Phase-Field Vesicle Membrane Model. *SIAM J. Sci. Comput.*, 40(6):A3982–A4006, 2018.

[15] Michel Crouzeix. Étude de la stabilité des méthodes de Runge–Kutta appliquées aux équations paraboliques. *Publications des séminaires de mathématiques et informatique de Rennes*, S4(3):1–6, 1974.

[16] Michel Crouzeix and Pierre-Arnaud Raviart. Méthodes de Runge–Kutta. Unpublished lecture notes, Université de Rennes, 1980.

[17] Michel Delfour, Michel Fortin, and Guy Payre. Finite-difference solutions of a nonlinear Schrödinger equation. *J. Comput. Phys.*, 44(2):277–288, 1981.

[18] Stéphane Descombes. Convergence of a Splitting Method of High Order for Reaction-Diffusion Systems. *Math. Comput.*, 70(236):1481–1501, 2001.

[19] Stéphane Descombes and Marc Massot. Operator splitting for nonlinear reaction-diffusion systems with an entropic structure: singular perturbation and order reduction. *Numer. Math.*, 97:667–698, 2004.

[20] Guillaume Dujardin. Exponential Runge–Kutta methods for the Schrödinger equation. *Appl. Numer. Math.*, 59(8):1839–1857, 2009.

[21] Guillaume Dujardin and Ingrid Lacroix-Violet. High order linearly implicit methods for evolution equations. *ESAIM, Math. Model. Numer. Anal.*, 56(3):743–766, 2022.

[22] Guillaume Dujardin and Ingrid Lacroix-Violet. $\hat{A}$- and $\hat{I}$- stability of Runge–Kutta collocation methods. *Appl. Numer. Math.*, 202:158–172, 2024.

[23] Angel Durán and Jesús M. Sanz-Serna. The numerical integration of relative equilibrium solutions. The nonlinear Schrödinger equation. *IMA J. Numer. Anal.*, 20(2):235–261, 2000.

[24] Pierre Grisvard. *Elliptic Problems in Nonsmooth Domains*. Society for Industrial and Applied Mathematics, 2011.

[25] Ernst Hairer. Constructive characterization of A-stable approximations to $\exp(z)$ and its connection with algebraically stable Runge–Kutta methods. *Numer. Math.*, 39(2):247–258, 1982.

[26] Ernst Hairer, Christian Lubich, and Gerhard Wanner. *Geometric Numerical Integration: Structure-Preserving Algorithms for Ordinary Differential Equations*, volume 31 of *Springer Series in Computational Mathematics*. Springer, 2nd ed edition, 2002.

[27] Marlis Hochbruck and Alexander Ostermann. Exponential Runge–Kutta methods for parabolic problems. *Appl. Numer. Math.*, 53(2):323–339, 2005. Tenth Seminar on Numerical Solution of Differential and Differntial-Algebraic Euqations (NUMDIFF-10).

[28] Marlis Hochbruck and Alexander Ostermann. Exponential integrators. *Acta Numer.*, 19:209–286, 2010.

[29] Christian Klein. Fourth order time-stepping for low dispersion Korteweg–de Vries and nonlinear Schrödinger equations. *Electron. Trans. Numer. Anal.*, 29:116–135, 2007.

[30] Hervé Ledret. Numerical Approximation of PDEs, 2011-2012. `https://www.ljll.math.upmc.fr/ledret/M1ApproxPDE.html`.

[31] Christian Lubich. On splitting methods for Schrödinger–Poisson and cubic nonlinear Schrödinger equations. *Math. Comput.*, 77(264):2141–2153, 2008.

[32] Christian Lubich and Alexander Ostermann. Linearly implicit time discretization of non-linear parabolic equations. *IMA J. Numer. Anal.*, 15(4):555–583, 1995.

[33] Yousef Saad. *Iterative Methods for Sparse Linear Systems*. Society for Industrial and Applied Mathematics, second edition, 2003.

[34] Jie Shen and Jie Xu. Convergence and Error Analysis for the Scalar Auxiliary Variable (SAV) Schemes to Gradient Flows. *SIAM J. Numer. Anal.*, 56(5):2895–2912, 2018.

[35] J. André C. Weideman and Ben M. Herbst. Split-Step Methods for the Solution of the Nonlinear Schrodinger Equation. *SIAM J. Numer. Anal.*, 23(3):485–507, 1986.